Anti-cancer activity of the fruit extract of *Ricinus communis* L. (RCFE) and identification of major compounds

4.1. Introduction

Medicinal plants are rich sources of bioactive molecules and can be exploited for application as anti-cancer agents [1-7]. In search of a novel medicinal plant-based therapeutic approach against breast cancer, fruit extract of *Ricinus communis* L. *(Euphorbiaceae)* obtained from the Golaghat district of Assam, India has been selected to study in detail. *R. communis* L, commonly known as castor plant, well-known for its traditional and medicinal use globally is abundant in North East India and distributed throughout Assam, Meghalaya, Nagaland along with other states of India like Bihar, Gujarat, Maharastra, Madhya Pradesh, Odisha, Rajasthan, Uttar Pradesh [8,9]. Various parts of this plant have been used for the treatment of pain, paralysis, constipation, gastritis, warts [10,11]. Ethanolic extract of the leaves has shown hepatoprotective effect in hepatocytes whereas 50% ethanolic extract of roots of these plants has shown anti-diabetic and reversible anti-fertility activity in *in-vivo* rat models [12-14]. A methanolic extract of the roots of same plant has shown anti-inflammatory in wister albino rats and free radical scavenging activity in *in-vitro* conditions [15]. There are other reports which indicate the effectiveness of this plant as an anti-fungal agent and also as a pest control measure [13,16-18]. A volatile extract from the leaves of the plants has shown to induce apoptosis in human melanoma cells (SK-MEL-28) [8]. However, a mechanistic study on the anti-cancer efficacy of the fruits of *R. communis* L. is not reported.

4.2. Classification of the plant

Kingdom: Plantae
Subkingdom: Tracheobionta
Superdivision: Spermatophyta
Division: Magnoliophyta
Class: Magnoliopsida
Subclass: Rosidae
Order: Euphorbiales
Family: Euphorbiaceae
Genus: *Ricinus* L.
Species: *Ricinus communis* L.

4.3. Materials and Methods

4.3.1. Cell lines and reagents

The cell lines MCF-7, MDA-MB-231, MDA-MB-453, ZR-75-1, HT-29, and A549 were purchased from NCCS Pune, India. MEF was a gift from Dr. Sougata Saha, Department of MBBT, Tezpur University, India. DMEM (Dulbecco's Modified Eagle Medium) and FBS (Fetal Bovine Serum) were purchased from Life Technologies, USA. MTT (3-(4, 5-dimethyl thiazolyl-2)-2, 5-diphenyltetrazolium bromide), Collagen IV, ECM gel and Doxorubicin were also purchased from Sigma Aldrich and Mitomycin C was purchased from HiMedia, India. Annexin-V-FLUOS Staining Kit purchased from Roche, USA and Annexin V FITC Assay Kit was purchased from Cayman, USA. Antibodies used in this study were procured from Cell Signalling Technology, USA.

4.3.2. Preparation of extract

Fresh fruits of the plant *Ricinus communis* L. were collected and morphological identification of the specimen was done at the Botanical Survey of India, Shillong, Meghalaya. The fresh fruits were extracted as discussed in **section 3.2.3. of chapter 3** and named RCFE.

4.3.3. Cell culture

MCF-7, MDA-MB-231, MDA-MB-453, ZR-75-1, HT-29, and A549 cell lines were routinely maintained in Dulbecco's modified Eagle's medium (DMEM; Gibco), and the medium was complemented with 10% fetal bovine serum and 1% antibiotic. Cell lines were kept in a CO_2 incubator at 5% CO_2 and 37^0 C temperatures.

4.3.4. Wound healing migration assay

Cells were seeded in a 24 well plate till 90% confluency. The media was replaced by FBS-devoid media for at least 6 hr and mitomycin C (1 ug/ml) was added before 1 hr of treatment to stop proliferation. Using a sterile pipette tip, a straight scratch was made simulating a wound in each of the wells. The extract at two nontoxic concentrations (0.05 and 0.1 µg/ml) was added and images were taken at 0, 24 and 48 hr following the treatment from at least 3 different fields of each well. The width of the wound was measured and quantified [19,20].

4.3.5. Collagen adhesion assay

To evaluate the efficacy of the extracts to inhibit adhesion, $2x10^5$ cells/ml were pre-treated with 0.05 and 0.1 µg/ml of extracts in serum-free media for 24 hr. Cells were trypsinized and resuspended in 1 ml 1% BSA containing DMEM. 200 µl cell suspension was plated in 96-well plates pre-coated with collagen IV and allowed to adhere for 60 min. The media was gently removed, and the wells were washed with PBS thrice. The attached cells were quantified using MTT [21].

4.3.6. Matrigel invasion assay

$2.5x10^5$ cells/well were plated in a 6 well plate with or without treatment (0.05 and 0.1 µg/ml of extracts) in a serum-free media for 24hr. Then cells were trypsinized and resuspended in 200 µl serum-free media and placed in the upper chamber of ECM gel pre-coated transwell inserts of pore size 8.0 µm, 6.5 mm diameter, and PET membrane. The lower chamber was filled with 10% FBS containing media to create a concentration gradient and incubated for 24 hr in the case of MCF-7 or 6 hr in case of MDA-MB-231. Then inserts were washed and cells were fixed with formaldehyde and permeabilized with methanol. The cells were then stained with Giemsa stain. Non-invasive cells were removed by scraping with a cotton swab and bright-field images of invasive cells were taken using an Olympus IX83 microscope. The cells were counted from photomicrographs of 10 random fields of a single membrane [22,23].

4.3.7. DNA fragmentation assay

Both MCF-7 and MDA-MB-231 cells were treated with RCFE (1 µg/ml) for 0, 24 and 48 hr. Cells were trypsinized and genomic DNA was isolated using PureLink™ Genomic DNA Mini Kit (Invitrogen, USA). Concentration was measured, and DNA was run on a 2% agarose gel [24].

4.3.8. Annexin V/PI apoptosis assay

20,000 cells/well were plated in a 96 well plate and allowed to seed overnight. The cells were treated with two different concentrations of the extract or Doxorubicin (1 µg/ml) followed by incubation for 24 hr. The media is removed carefully and Annexin V/PI is added according to the manufacturer's protocol of Annexin-V-FLUOS Staining Kit (Roche, USA), incubated for 15 min and fluorescent images were taken from five

different fields of each well using fluorescence microscope (Model Olympus IX83, Japan).

4.3.9. Flow cytometer analysis for apoptosis

MCF7 and MDA-MB-231 cells ($1x10^5$ cells/well) were seeded in 12 well culture plates and incubated overnight. Then adhered cells were treated with RCFE 0.5 µg/ml and 1 µg/ml for 24 hr. After incubation, both floating as well as adherent cells from each well were collected in tubes and washed with PBS. The cell pellets were resuspended in 200 µL of binding buffer and required proportions of FITC-Annexin V/ PI were added to each sample according to manufacturer's protocol of Annexin V FITC Assay Kit (Cayman, USA). The samples were incubated in dark for 15 min and analyzed with FACSChorus software on a FACS Melody flow cytometer (BD Biosciences).

4.3.10. Western blot analysis

Cells were seeded in a 100 mm dish at $1x10^6$ cells per dish and incubated overnight before treating with the indicated concentrations for 24 hr. Proteins were extracted from RCFE and doxorubicin (positive control) treated MCF-7 and MDA-MB-231 cells with ice-cold RIPA buffer (Thermo Scientific, USA) containing protease and phosphatase inhibitor cocktail (Thermo Scientific, USA). An equal amount of proteins from different experimental samples was run in SDS-PAGE and proteins were transferred to a PVDF membrane using a semidry electrophoresis transfer unit (GE Healthcare, UK). After blocking with 3% BSA in TBS-Tween 20 for at least 1 hr at room temperature, the membranes were probed with the corresponding primary antibodies viz. GAPDH (cat# BB-AB0060), p53 (cat# BB-AB0100) from BioBharati LifeSciences Pvt. Ltd. and β-actin (cat#4970), MMP-2 (cat#4022), MMP-9 (cat#3852), Bcl-2 (cat#2870), Bax (cat#2772), PARP (cat#9532), Caspase7 (cat#9492), CyclinE1 (cat#4129), STAT3 (cat#9139) and p-STAT3 (cat#9145) from Cell Signaling Technology, Inc. (1:1000 dilutions). This was followed by incubation with secondary antibodies (Anti-Rabbit, Cat#8889 and Anti-Mouse Cat#8890, Cell Signaling Technology, Inc.) for 1 hr at room temperature. The blots were then incubated with chemiluminescence substrate (cat# 1705061, Bio-Rad, USA) and bands were visualized using Chemidoc XRS+ imaging system (Bio-Rad, USA). Quantification of the bands was done using Gel Quant software.

4.3.11. Syngeneic mouse model to study inhibition of tumorigenesis by RCFE

Female Balb/c mice were procured from Center for Translational Animal Research (CTAR), Bose Institute, Kolkata, India and maintained as per the guidelines of the 'Committee for the Purpose of Control and Supervision of Experiments on Animals (CPCSEA). Mouse triple-negative breast cancer cells, 4T1 were cultured in DMEM media and the cytotoxic effect of RCFE on this cell line was determined by MTT assay as described in section **3.2.5. of chapter 3.** For *in vivo* tumorigenic assay, 4T1 cells (1×10^6 cells/animal) were subcutaneously injected into the mammary fat pad of 6-8 weeks old Balb/c mice to develop solid tumors. Animals which developed solid tumors were distributed into two groups randomly, each containing ten animals. One group was treated with 0.9 % normal saline (vehicle control) whereas, other group was subjected to intraperitoneal injection of RCFE (0.5 mg/kg) starting after 10 days of tumor development and continued until 22 days (4 doses, each at 72 hr interval). Tumor progression was monitored by measuring the volume of the tumor with vernier calipers on every third day. The tumor volume was calculated by using the formula "$\mathbf{V = 0.5 \times a \times b^2}$" where "a" and "b" indicate length and width diameter, respectively. The experimental protocol was approved by the animal ethics committee of Bose Institute (Ref. No. IAEC/BI/87/2017, dated Dec. 13, 2017) registered with the CPCSEA.

4.3.12. Fractionation of the extract

The dried powdered plant material was first defatted by extracting with 3-4 liter petroleum ether at least three times by cold maceration process. After each step, the solvent was filtered out by using filter paper so as to remove dirt and small plant particles. The solvent was then evaporated. After removing the solvent the remaining plant material was subjected to hydro-alcoholic extraction (1: 1:: Alcohol: water) at room temperature in 3-4 liter solvent system at least five times for 48 hr. After each step, the extract was filtered with a Whatman filter paper. After this, the filtered extracts were combined and lyophilized to generate the crude hydro-alcoholic extract. After keeping some of the extracts for bioactivity the remaining extract was then suspended in milli-Q water and partitioned successively with 1-2 liter EtOAc, at least six times and 1-2 liter *n*-BuOH, at least six times at 60–90 °C. Each fraction was evaporated and lyophilized to yield the EtOAc fraction [RC(E)], *n*-BuOH fraction

[RC(B)] and aqueous fraction [RC(A)]. All the fractions were stored at 4^{o}C and checked for the biological activity.

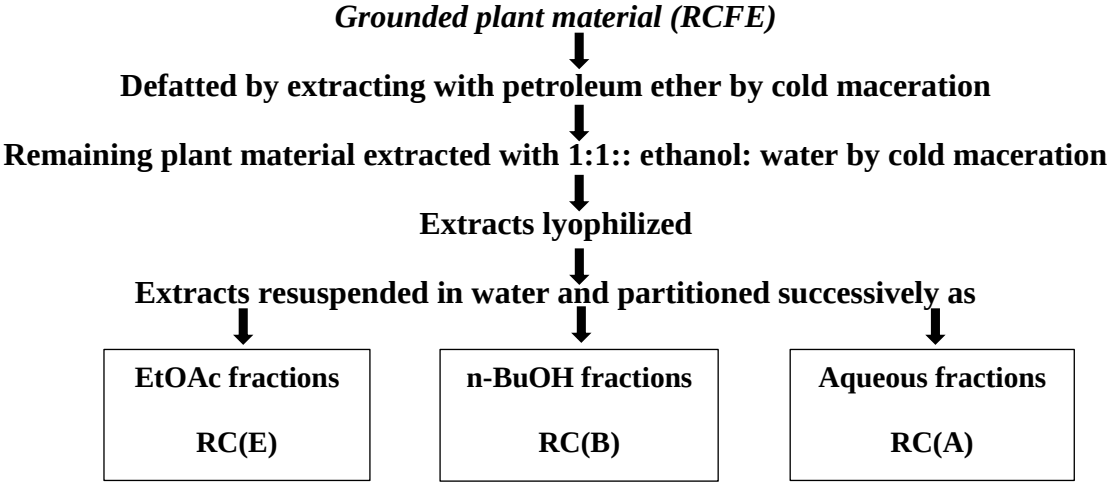

4.3.13. Cytotoxicity assessment of the extract and fractions

In this assay cells (5000 cells/well) were plated in a 96 well plate and incubated for 48 hr. Cells were treated with different concentrations of either crude or different fractions of RCFE followed by further incubation of 24 or 48 hr and quantified as depicted in **section 3.2.5. of chapter 3**.

4.3.14. Fingerprint analysis of R. Communis L. fruit extracts

HPLC and ESI-MS techniques were used to identify the phytochemicals present in the *R. Communis* L. extracts. HPLC fingerprint analysis was performed at 25±1^{o}C using ethyl acetate fraction of *R. Communis* L. which was dissolved in acetonitrile solvent and filtered through membrane filters (0.45 µm pore size). The sample (20 µL injected volume) was analyzed using a Shimadzu system (Kyoto, Japan) equipped with LC-20AT Prominence liquid chromatography pump, DGU-20A$_3$ Prominence Degasser, CBM-20A Prominence communications bus module, SPD-20A Prominence UV/VIS detector, LC solution software, and a Rheodyne injector with 100 µL loop. Separation was achieved using Phenomenex RP C18 column, 250 × 4.6mm, 5 µm; a gradient mobile phase consisted of water (A) and acetonitrile (B) with a gradient elution program, i.e., 0–40 min, 80-50% B; 40–70 min, 50-0% B; 70–80 min, 0% B; 80–90 min, 0-90% B and 90–100 min 80% B, flow 1 mL/min. The elute was monitored at 210

nm and 254 nm. Mass analysis of the major HPLC peak was recorded on Agilent 6540 Q-TOF LC/MS system.

4.3.15. Biological activity of pure compounds

To evaluate the cytotoxicity of four compounds identified from RCFE, MCF-7 and MDA-MB-231 cell lines were treated with increasing concentrations of the Ricinine, p-Courmaric acid, Epigallocatechin and Ricinoleic acid for 24 hr and the effect were determined by MTT assay as described in **section 3.2.5. of chapter 3**. To determine the effect of these compounds on migration and adhesion *in vitro* wound healing migration assay and collagen adhesion assay was done using two non-toxic concentrations of the compounds as depicted in **section 4.3.4 and 4.3.5**.

4.3.16. Statistical analysis

Statistical analysis was performed using Graph Pad Prism and data were expressed as mean± standard deviation (mean± SD). Results were analyzed either by two-way analysis of variance (two-way ANOVA) or one-way analysis of variance (one-way ANOVA) or Student's t-test as required by the experimental system and differences were considered to be significant at $p<0.05$.

4.4. Results

4.4.1. RCFE inhibits migration of MCF-7 and MDA-MB-231 cells

To understand the role of RCFE on the metastatic properties of breast cancer, its effect on the migration of MCF-7 and MDA-MB-231 cells *in vitro* were studied using wound-healing assay. RCFE treatment for 24 and 48 hr demonstrated dose-dependent inhibition of migration in both cells **(Fig 4.1.A and 4.1.B)**. The inhibition of migration in response to 0.05 µg/ml of RCFE after 24 hr was not significant in MCF-7 cells. However, the same concentration was sufficient to inhibit migration significantly after 48 hr. The effect was highly significant when MCF-7 cells were treated with a higher concentration of RCFE (0.1 µg/ml) even at 24 hr. Interestingly, the effect of RCFE on inhibition of migration was robust on highly metastatic MDA-MB-231 as shown by significant inhibition of migration in these cells after treatment with both the doses for 24 and 48 hr **(Fig. 4.1.B)**.

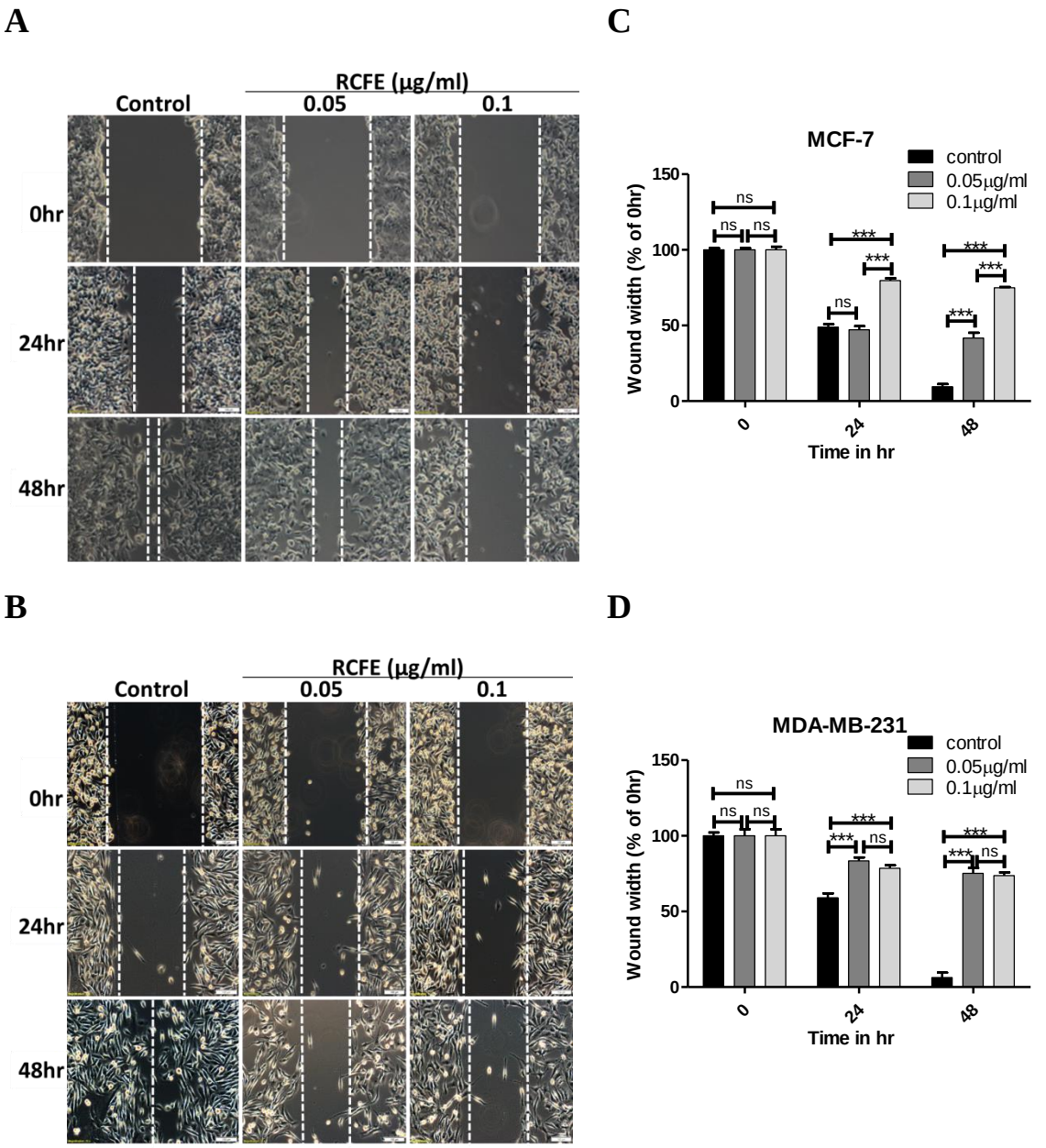

Figure 4.1.: RCFE inhibited the migration of breast cancer cells. Inhibition of migration of MCF-7 **(A)** and MDA-MB-231 **(B)** with the treatment of 0.05 and 0.1 µg/ml for 24 and 48 hr. The quantification of wound widths as shown in right panels. Data represent the mean ± SEM of three independent experiments. Statistical differences were analyzed with two-way ANOVA test. p-value ns>0.05, p-value ***<0.0001.

4.4.2. Effect of RCFE on adhesion of MCF-7 and MDA-MB-231 to collagen IV

The ability to adhere to extracellular matrices is one of the hallmarks of metastatic cancer cells. Pre-treatment of both MCF-7 and MDA-MB-231 cells with two concentrations of RCFE demonstrated a significant reduction in the adhesion of the cells to collagen IV coated wells in a dose-dependent fashion **(Fig 4.2.A and 4.2.B)**.

Treatment with 0.05 µg/ml and 0.1 µg/ml RCFE inhibited adherence by 21% and 41% in MCF-7 cells and 22% and 40% in MDA-MB-231 cells, respectively.

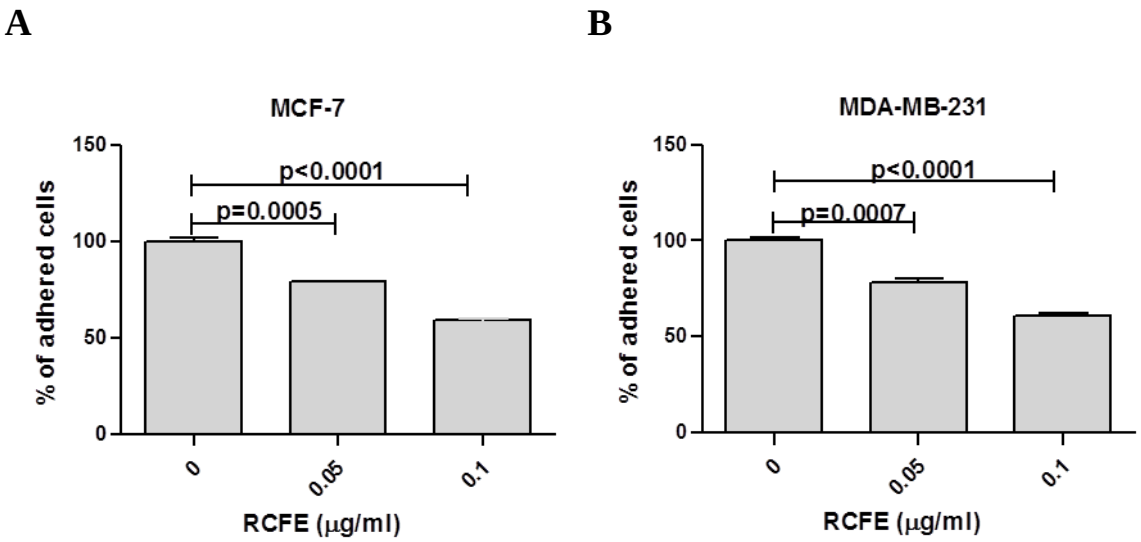

Figure 4.2.: RCFE inhibits adhesion of MCF-7 and MDA-MB-231 cells. Effect of RCFE on adhesion of MCF-7 **(A)** and MDA-MB-231 **(B)**. Data represented as mean ± SEM of three independent experiments. Statistical differences were analyzed with a one-way ANOVA test. p-value <0.05 was considered significant.

4.4.3. RCFE retards invasion of MCF-7 and MDA-MB-231 cells to matrigel

Further, the effect of RCFE on the invasion of the two breast cancer cells was studied *in vitro* condition. Cells pre-treated with or without RCFE were allowed to invade through extracellular matrix (ECM) gels in response to a 10% FBS-containing medium. In MCF-7 cells, treatment with 0.05 and 0.1 µg/ml of RCFE reduced 42% and 66% invasion compared to control cells after 24 hr **(Fig 4.3.A & 4.3.C)**. Interestingly again, the effect was more prominent in MDA-MB-231 cells as treatment with these two concentrations of RCFE led to 45% and 81% reduction in invasion after 6 hr **(Fig 4.3.B & 4.3.D)**.

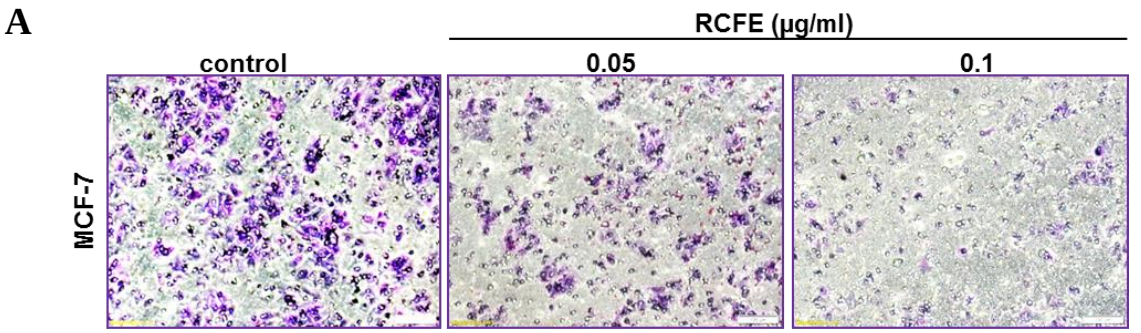

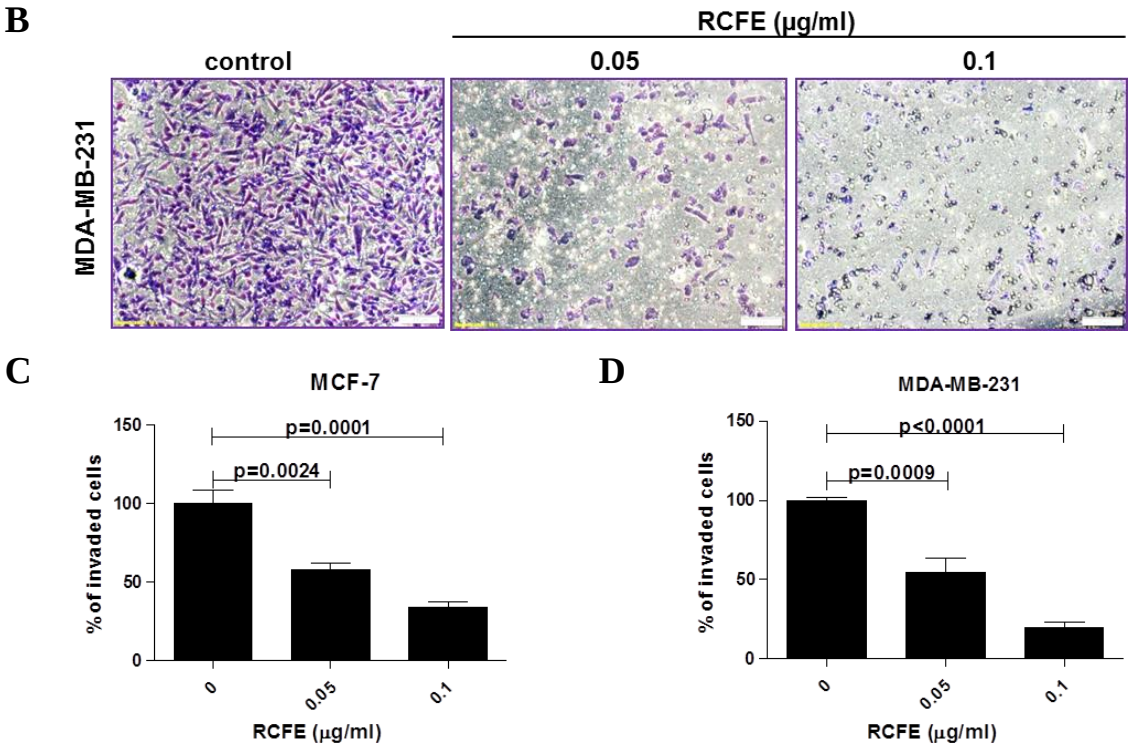

Figure 4.3.: RCFE inhibits the invasion of MCF-7 and MDA-MB-231 cells. Invasion of MCF-7 **(A)** and MDA-MB-231 **(B)** cells through ECM gel-coated transwell inserts in response to RCFE. Data represent the mean ± SEM of five different images of an individual set of three independent experiments **(C & D).** Statistical differences were analyzed with student t-test. p value<0.05 was considered significant.

4.4.4. RCFE down-regulates expression of MMPs in MCF-7 and MDA-MB-231 cells

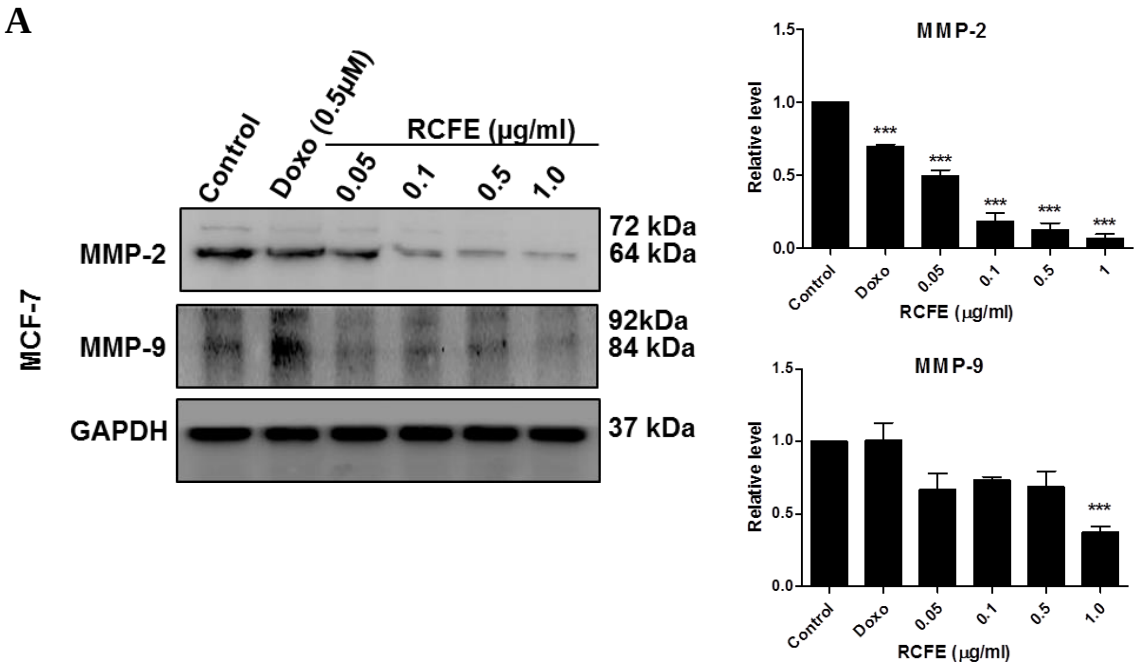

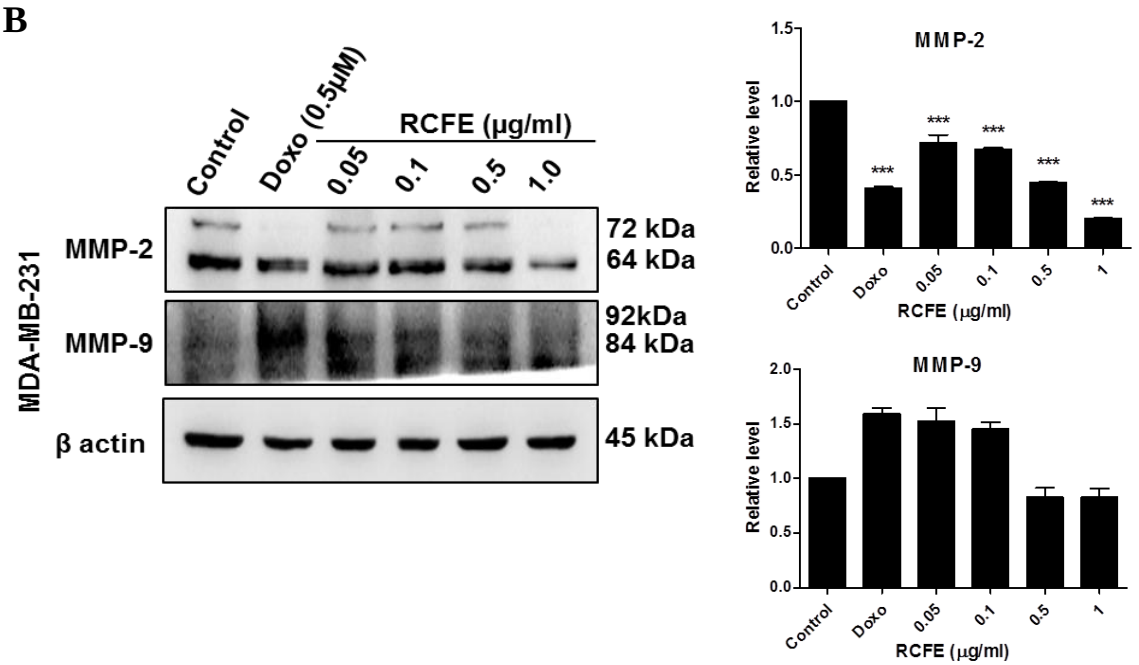

Figure 4.4.: RCFE treatment down-regulates MMPs expression. Western blot analysis of MMP-2 and -9 in MCF-7 **(A)** and MDA-MB231 **(B)** cells in response to treatment with RCFE. Doxorubicin (Doxo) has been used as a positive control. The quantitation of band intensities was represented in the right panels. Statistical differences were analyzed with one-way ANOVA test. p-value <0.05 was considered significant

Matrix metalloproteinases (MMPs) act as a facilitator of cancer cell invasion and thus plays key role in metastasis. MMPs degrade the extracellular matrix (ECM) that helps the cells to overcome barriers for invasion into other organs. They also help in modulating cell-cell adhesion. Western blot analysis suggested treatment of RCFE for 24 hr reduced expression of MMP-2 and MMP-9 in MCF-7 and MDA-MB-231 cells in a concentration-dependent manner **(Fig 4.4.A and 4.4.B)**. RCFE at a concentration of 1.0 µg/ml reduced the MMP-2 expression by about 10 folds in MCF-7 cells and 4 folds in MDA-MB-231 cells. Treatment with the same concentration of RCFE led to approximately 2 folds reduction in expression of MMP-9 in MCF-7 cells. However, no significant changes in its expression were found in MDA-MB-231 cells treated with 1.0 µg/ml of RCFE.

4.4.5. RCFE induced apoptosis in MCF-7 and MDA-MB-231 cells

Since the induction of apoptosis is a well-characterized mode of controlling cancer cell proliferation by an anti-cancer agent; we next studied the role of RCFE in inducing apoptosis in two cell lines. Genomic DNA isolated from the cells following treatment with 1.0 µg/ml RCFE for 24 and 48 hr demonstrated DNA degradation **(Fig 4.5.A)**,

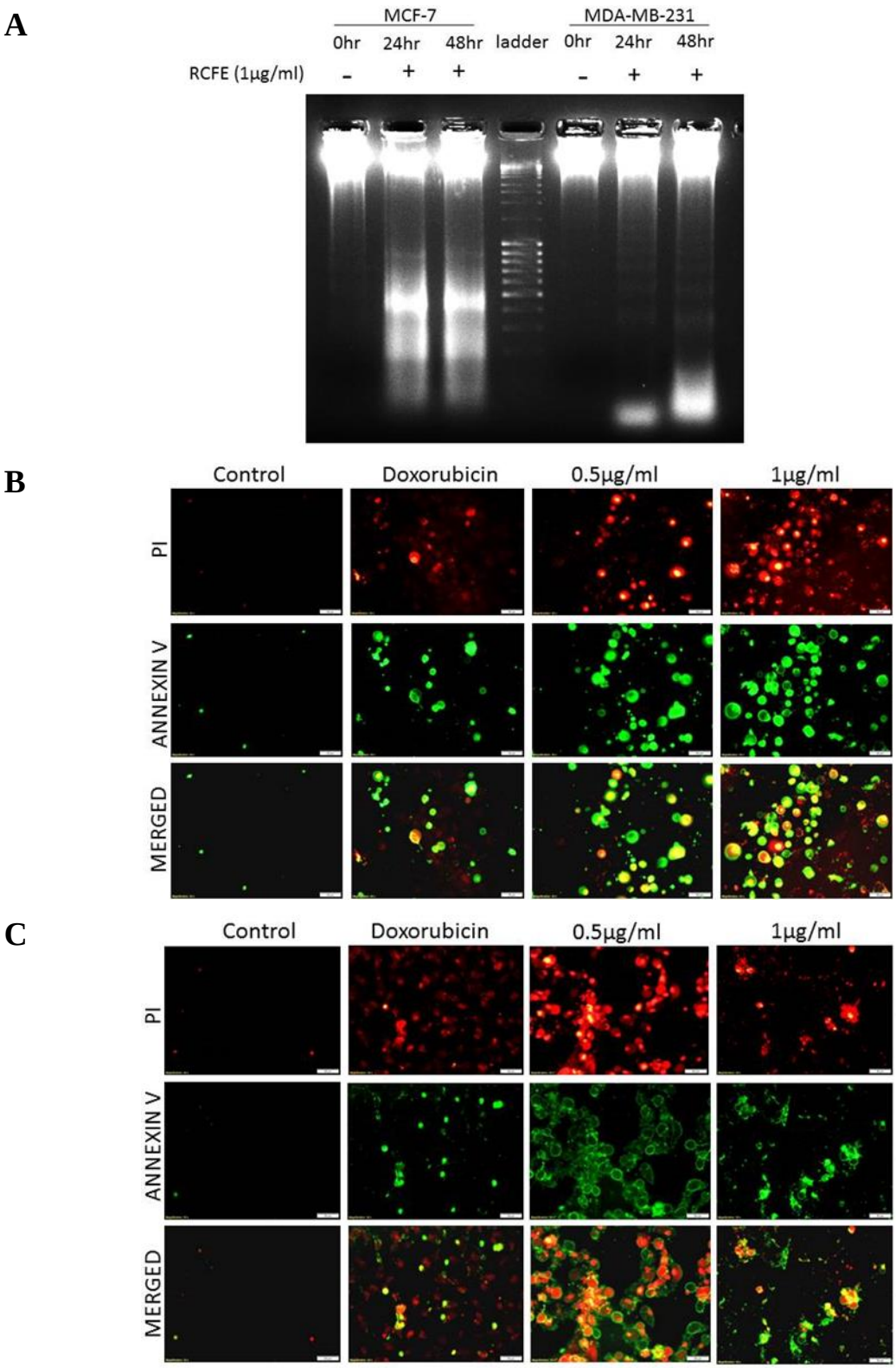

Figure 4.5.: RCFE induced apoptosis in MCF-7 and MDA-MB-231 cells. The DNA fragmentation was observed in RCFE (1µg/ml) treated MCF-7 and MDA-MB-231 cells in 24 and 48 hr on 2% Agarose gel electrophoresis **(A)**. Annexin V/PI stained images of MCF-7 **(B)** and MDA-MB-231**(C)** cells were taken at 488 nm and 594 nm. Doxorubicin has been used as a positive control. Representative images of propidium iodide (top panels) and Annexin V (middle panels) stained cells are presented along with the merged images (bottom panels).

which indicated the induction of apoptosis in the cells. To confirm the induction of apoptosis by RCFE, Annexin V/PI assay was performed which showed the cells were going through apoptosis after treatment with the extract **(Fig 4.5.B & 4.5.C)**. In general green fluorescence indicates early apoptosis in the cells as exposure of membrane phospholipid phosphatidylserine (PS) to the extracellular environment prompts its binding to Annexin V. The red fluorescence is generated by cells that are dead or in late stage of apoptosis and therefore, their membrane becomes permeable to PI. Treatment of RCFE induced apoptosis to both MCF-7 and MDA-MB-231 cells. Treatment with low dose of RCFE (0.5 µg/ml) demonstrated higher number of cells with properties of early apoptosis in comparison to treatment with higher dose (1 µg/ml) **(bottom panels; Fig 4.5.B and 4.5.C)**. In later cases, most cells appeared in their late apoptotic stage. This experiment pointed towards apoptosis-inducing efficacy of RCFE in both experimental cells.

To quantify the percentage of apoptotic cells flow cytrometric analysis was performed with cells treated with 0.5 and 1.0 µg/ml RCFE for 24 hr **(Fig 4.6.A and 4.6.B)**. In MCF-7 cells, both the treatments induced more than 3 folds augmentation in apoptosis (early and late). The increase in apoptosis in MDA-MB-231 cells was found to be 2.7 folds at 0.5 µg/ml and 11 folds at 1.0 µg/ml RCFE treatment, respectively **(Fig 4.6.C and 4.6.D)**.

To understand the signaling mechanism of RCFE-induced apoptosis in MCF-7 and MDA-MB-231 cells, the expression level of apoptosis-associated proteins like Bax, Bcl-2, PARP, and Caspase-7 were studied by western blot **(Fig 4.7.A and 4.7.B)**. Treatment with RCFE augmented expression of apoptotic protein Bax and concomitantly inhibited anti-apoptotic protein Bcl-2 expression in a concentration-dependent manner in both the experimental cells. This led to an increase in Bax/Bcl-2 ratio, a critical indicator for cells undergoing apoptosis **(Fig 4.7.A and 4.7.B)**. Bcl-2 inhibition leads to the release of cytochrome c from the mitochondrion which induces the caspase pathway. Treatment with RCFE increased the expression level of caspase-7 in a dose-dependent manner suggesting the onset of apoptosis in the cells. A significant increase in caspase-7 level was found in cells treated with higher concentrations of RCFE **(Fig 4.7.A and 4.7.B)**. PARP, a DNA repair enzyme, is a substrate of caspases and increase in PARP cleavage as a result of RCFE treatment confirmed caspase-

mediated apoptosis in both MCF-7 and MDA-MB-231 cells **(Fig 4.7.A and 4.7.B)**.

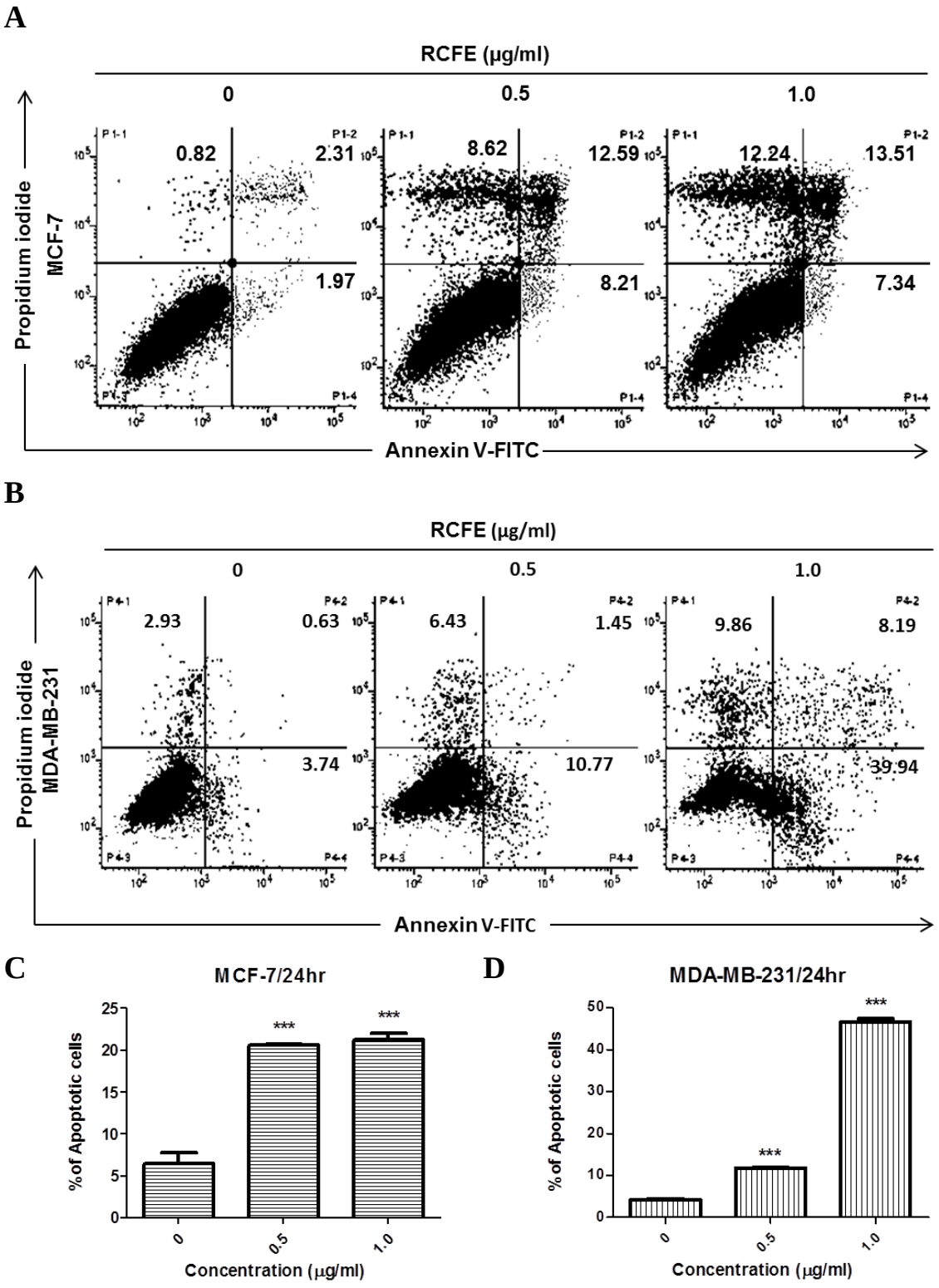

Figure 4.6.: Flow cytometer analysis of induction of apoptosis by RCFE in MCF-7 **(A)** and MDA-MB-231 **(B)** using Annexin V/PI. The quantitation of three independent analysis was presented in the right panels.

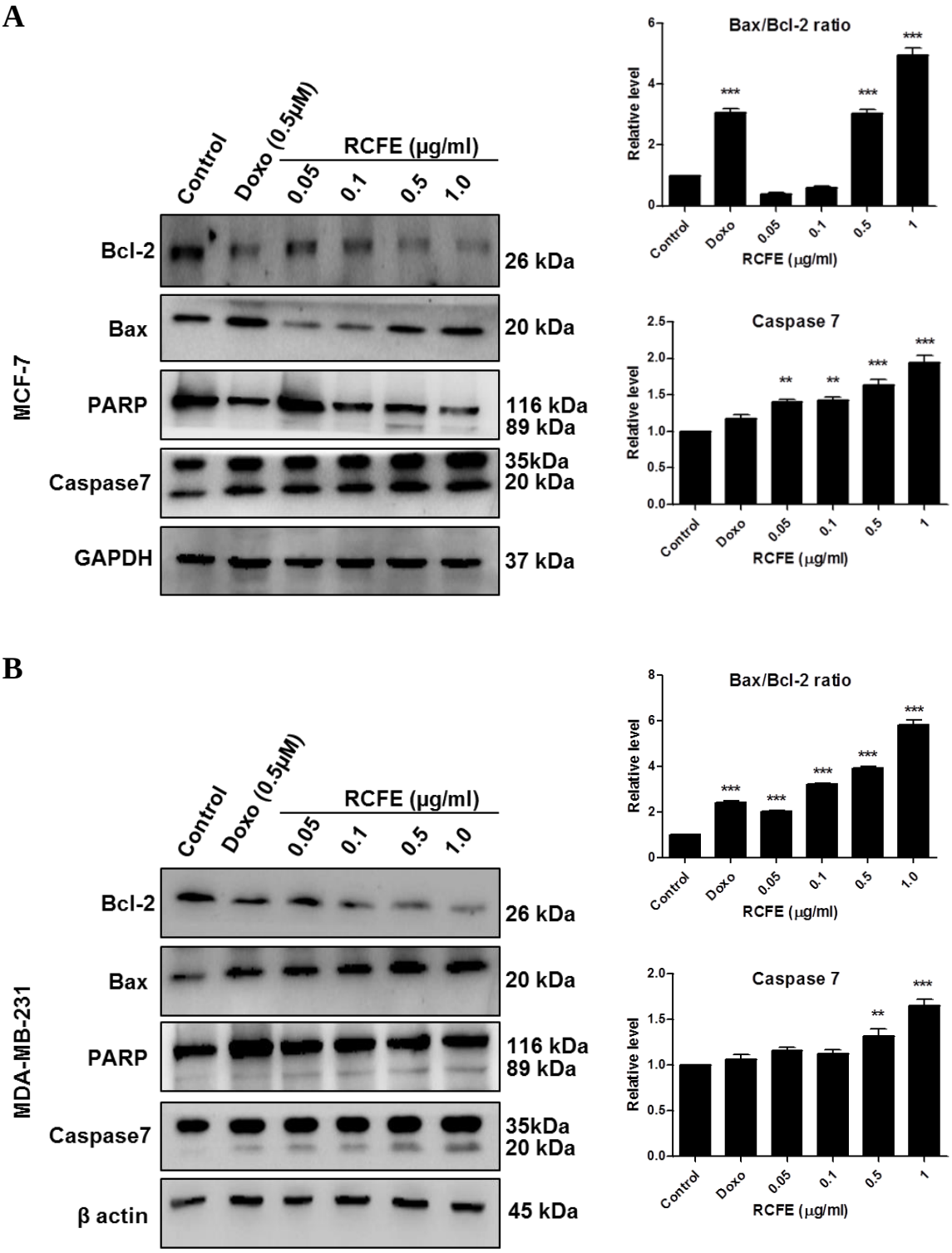

Figure 4.7.: Western blot analysis of induction of apoptosis in lysates from MCF-7 **(C)** and MDA-MB-231 **(D)** with antibodies against Bcl-2, Bax, PARP and Caspase-7. Doxorubicin (0.5 μM) was used as a positive control. GAPDH and β-actin are used as loading controls. The ratio of Bax/Bcl-2 and caspase-7 expressions were normalized either to GAPDH or β-actin presented in the lower panels. Statistical differences were analyzed with a one-way ANOVA test. p-value <0.05 was considered significant.

Expression of tumor suppressor gene p53 was also studied as the activation of p53 was proposed to play a key role in cell cycle arrest and apoptosis [25]. Treatment with RCFE did not show any activation of p53 in the cells suggesting the RCFE-induced apoptosis in these cells was possibly independent of p53 **(Fig 4.8.A and 4.8.B)**.

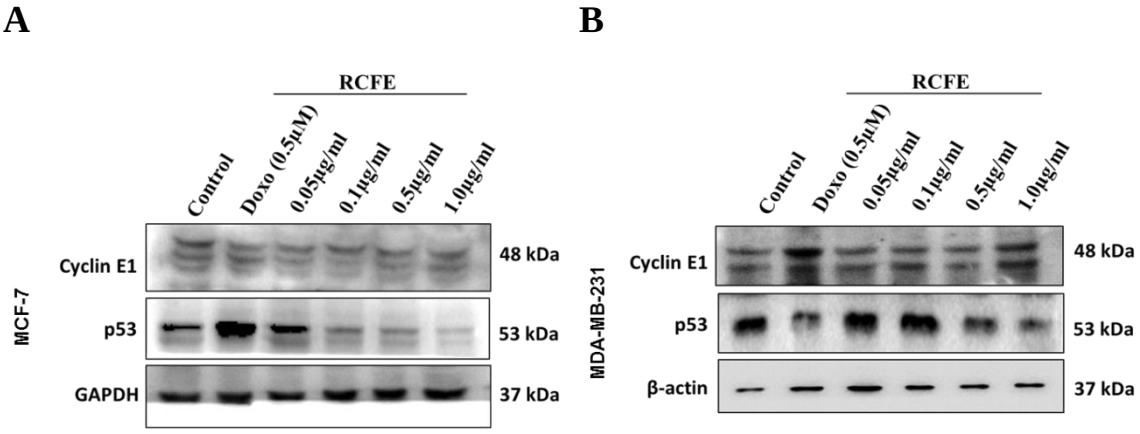

Figure 4.8.: Effect of RCFE on Cyclin E1 and p53 expression. MCF-7 **(A)** and MDA-MB-231 **(B)** cells were treated with various concentrations of RCFE and expression of Cyclin E1 and p53 were studied using western blots. Doxorubicin (Doxo) has been used as a positive control.

To understand if cell cycle arrest was also involved in the anti-cancer activity of RCFE, the expression of Cyclin E1 was studied. In both MCF-7 and MDA-MB-231 cells, the expression of Cyclin E1 did not change significantly with increased concentration of RCFE suggesting cells were not arrested in G1/S phase **(Fig 4.8.A and 4.8.B)**.

4.4.6. RCFE inhibits phosphorylation of STAT3

JAK-STAT pathway is involved in the activation of proteins related to apoptosis and metastasis including Bcl-2 and MMP2/9. We investigated the status of STAT3 phosphorylation in these cells followed by RCFE treatment. Treatment with an increasing concentration of RCFE significantly reduced phosphorylation at Tyr705 of STAT3; however, no alteration in the total STAT3 protein level was observed **(Fig 4.9.A and 4.9.B)**. The reduction in STAT3 phosphorylation was more evident in MCF-7 cells as treatment with 1 µg/ml RCFE almost abolished the phosphorylation. In MDA-MB-231 cells, reduction of STAT3 phosphorylation was observed only in the cells treated with higher concentrations (0.5 and 1.0 µg/ml) of RCFE. All the above observations pointed towards the coordinated role of RCFE in the induction of apoptosis and reduction of metastasis in breast cancer cells.

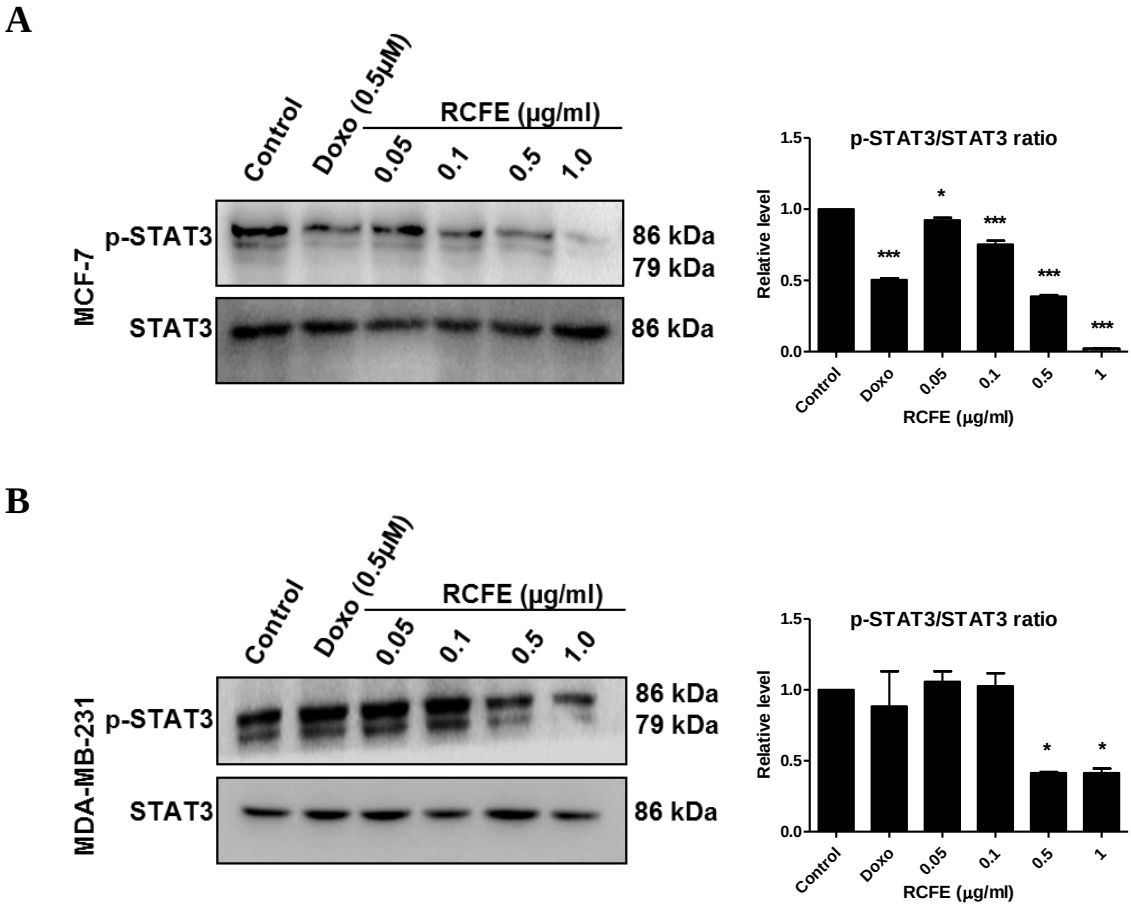

Figure 4.9.: RCFE treatment led to the dephosphorylation of STAT3. Western blot analysis of MCF-7 **(A)** and MDA-MB-231 **(B)** cell lysates with phosphor-STAT3 (Tyr705) and STAT3 antibodies. Doxorubicin (Doxo) has been used as a positive control. The quantitation of the expression was presented in the right panels. Statistical differences of three independent experiments were analyzed with a one-way ANOVA test. p-value <0.05 was considered significant.

4.4.7. RCFE inhibits tumor growth in a syngeneic mouse model

To understand the effect of RCFE on the progression of *in vivo* breast tumors, transplantable mouse mammary carcinoma cell 4T1 induced syngeneic model was studied. RCFE showed significant cytotoxicity against these cells *in vitro* as shown in figure **(Fig 4.10.A)**. The IC_{50} value of RCFE in 24 hr treatment in 4T1 cells was found to be 0.5 μg/ml and hence 0.5 mg/kg body weight is considered for further treatment in mice. The tumor was induced in female Balb/c mice by subcutaneous injection of 4T1 cells in the mammary fat pad. After 10 days, intraperitoneal administration of 4 doses of RCFE (at 0.5 mg/kg bodyweight concentration) was given to one set of animals, while the other set of animals received only vehicle (0.9% saline). The tumor continued to increase in the control group while RCFE treated animals showed significant reduction

in tumor volume with time **(Fig 4.10.B & 4.10.C)**. The volume of the dissected tumors from the sacrificed animals at 22 days following 4T1 injection were measured with vernier calipers **(Fig 4.10.D)**. RCFE-treated animals showed more than 88% reduction in tumor volume compared to control group animals **(Fig 4.10.E)**.

A

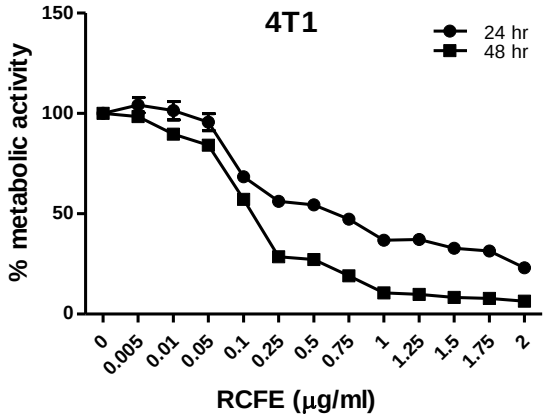

B **Untreated control**

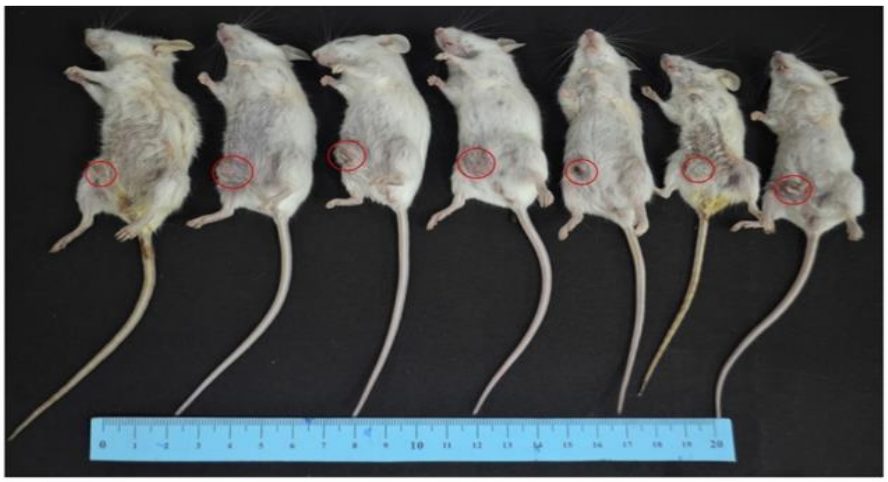

C **RCFE 0.5mg/kg body weight**

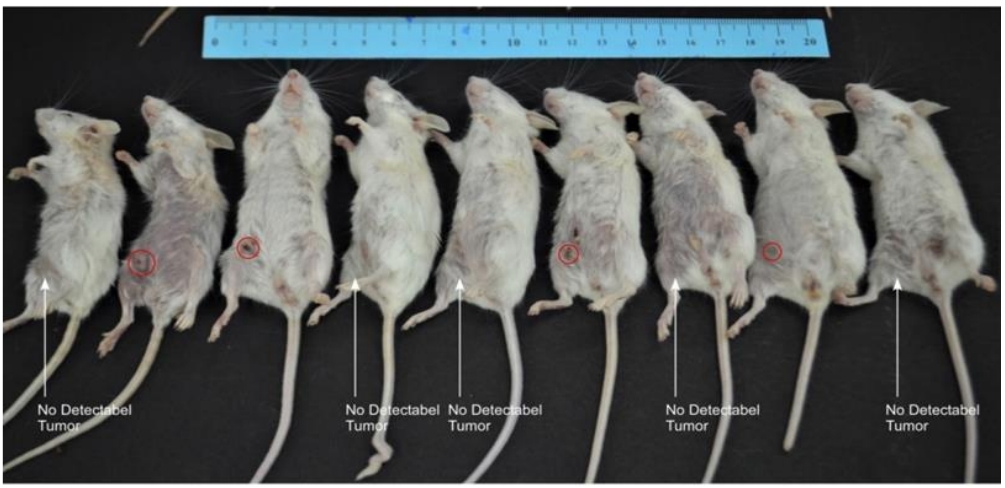

D

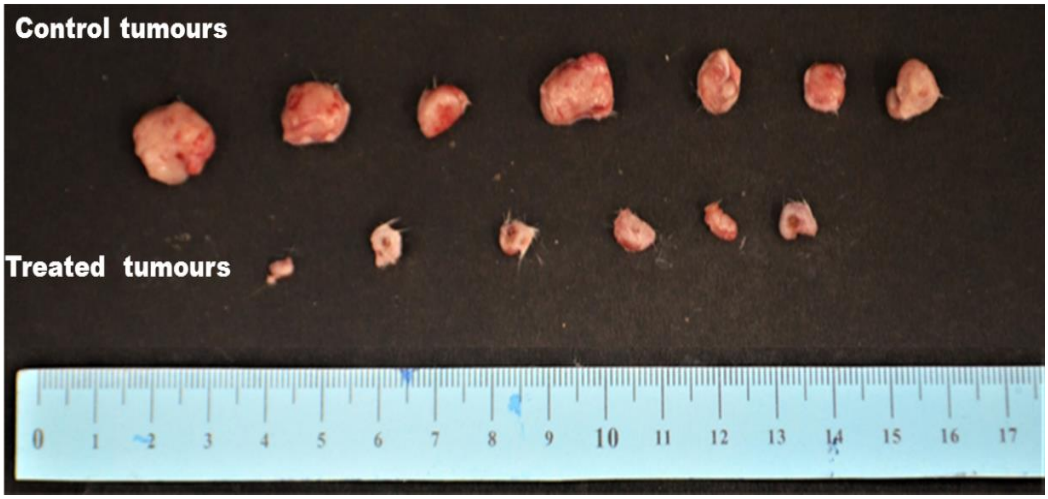

E

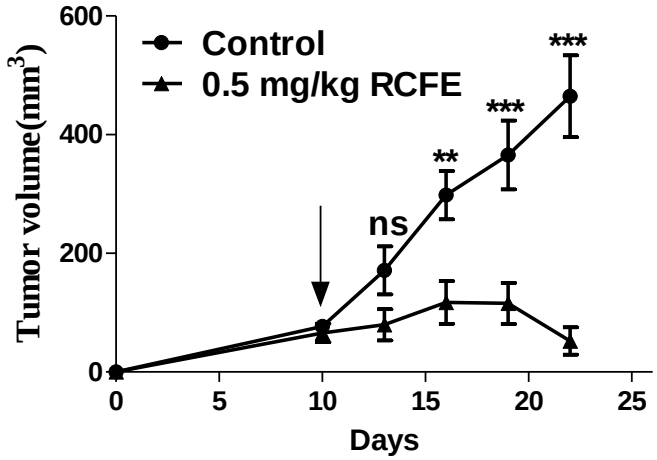

Figure 4.10.: Effect of RCFE on syngeneic mouse model. **(A)** 4T1 cells were treated with various concentrations of RCFE for 24 and 48 hr. Data represent the mean ± SEM of three independent experiments. The animals treated with 0.9% normal saline **(B)** and RCFE at 0.5 mg/kg body weight **(C)**. Animals with visible tumors from outside were pointed with red circles. Animals with no visible tumors from outside were shown by white arrows. The excised tumors from control and RCFE-treated animals **(D)** were measured and graph represented the tumor volumes in two different treatments **(E)**. Statistical differences were analyzed with two-way ANOVA test. p-value ns>0.05, p-value ***<0.0001.

4.4.8. Effect of RCFE on other cancer cells

After establishing the mechanism of anti-cancer activity of RCFE primarily using two breast cancer cell lines MCF-7 and MDA-MB-231, we decided to study the specificity of RCFE against additional cancer cell lines. For this purpose, four cell lines were selected viz HER2-positive MDA-MB-453 and triple-positive ZR-75-1 breast cancer cells, colon cancer cell line HT-29 and lung adenocarcinoma cell line A549. Amongst these, MDA-MB-453 and ZR-75-1 breast cancer cells showed 36.2% and 54.3% cell

death when treated with 1 µg/ml RCFE for 48 hr. Similar treatment demonstrated significant cytotoxicity of 64% in HT-29 and 54.2% in A549 after 48 hr **(Fig 4.11.A-D)**.

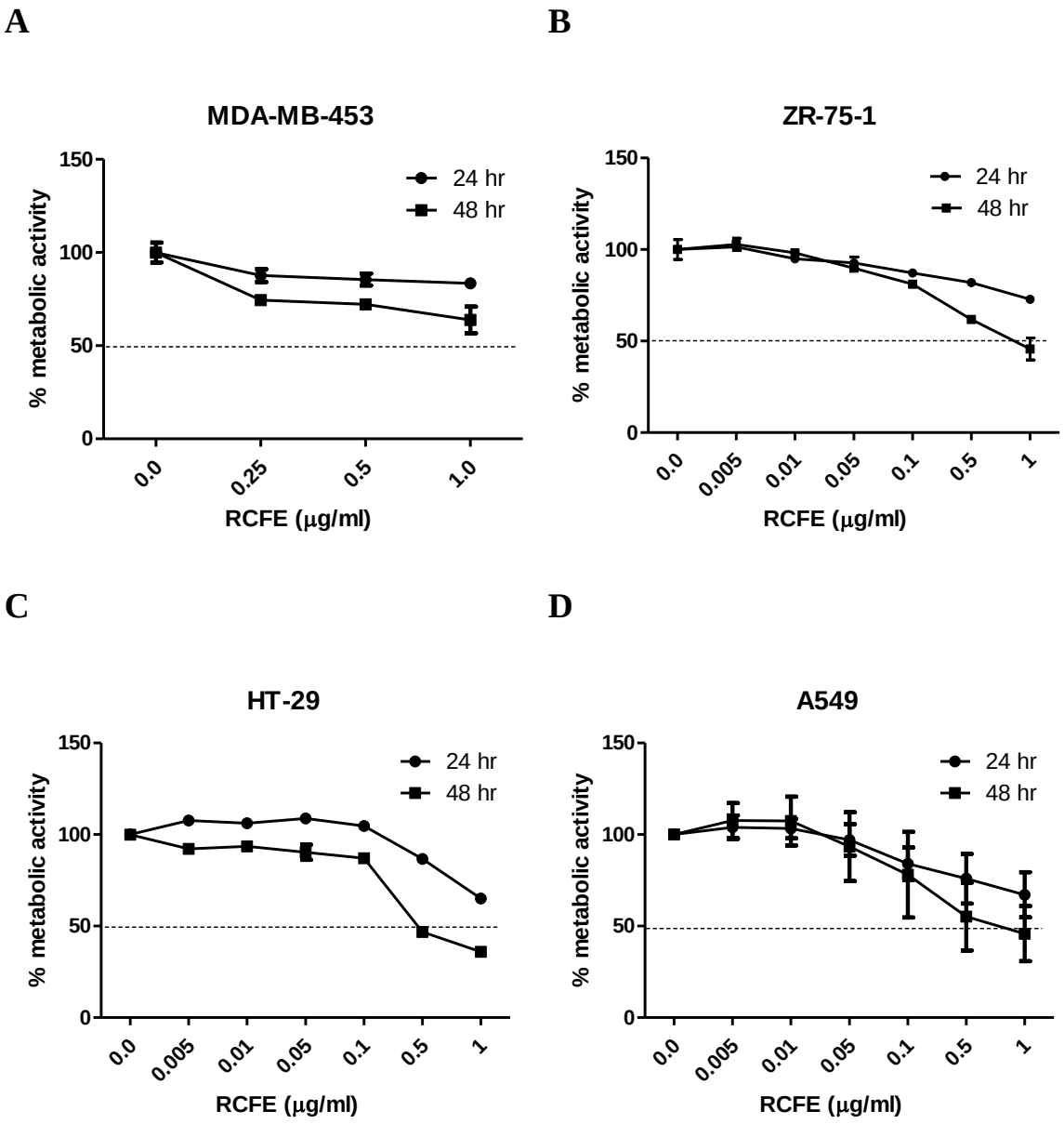

Figure 4.11.: **RCFE induced cytotoxicity in MDA-MB-453, ZR-75-1, HT-29, and A549 cells.** RCFE induced cytotoxicity in MDA-MB-453 **(A)** ZR-75-1 **(B)** HT-29 **(C)** and A549 **(D)** cells treated with various concentrations of RCFE for 24 and 48 hr. Data represent the mean ± SEM of three independent experiments.

As HT-29 and A549 also showed significant cytotoxicity when treated with RCFE, we next decided to study the expression of apoptosis regulating proteins in these cells following treatment with the extract. Treatment with increasing concentrations of RCFE induced the ratio of Bax/Bcl-2 expressions in both these cells along with increased

PARP cleavage **(Fig 4.12.A and 4.12.B)**. These observations suggested that RCFE could also induce apoptosis in cancer cells other than breast origin.

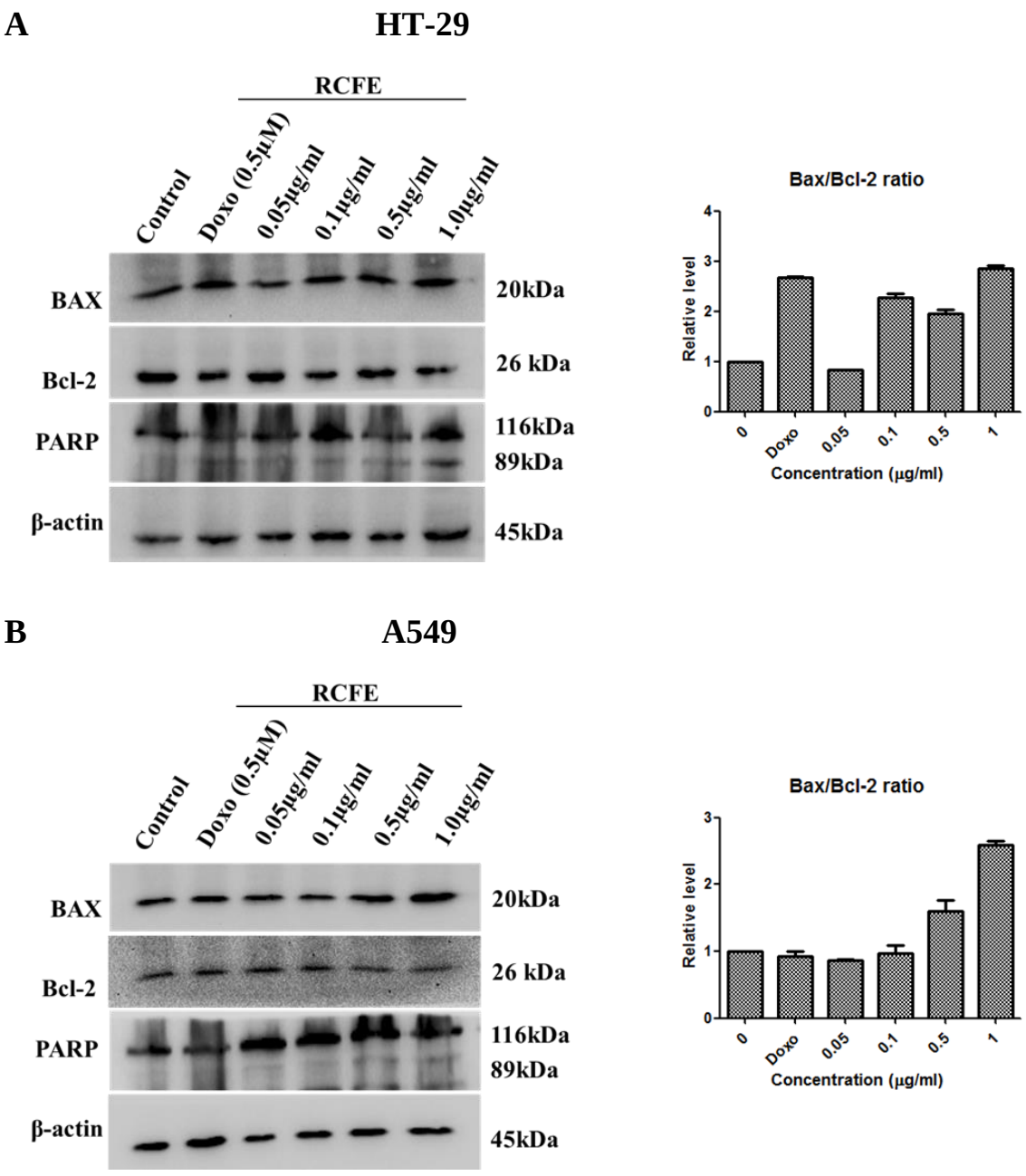

Figure 4.12.: RCFE induced apoptosis in HT-29 and A549 cells. For western blot assay HT-29 **(A)** and A549 **(B),** cells were treated with indicated doses of RCFE for 24 hr and protein extracted were used against with indicated antibodies. Doxorubicin (0.5µM) was used as a positive control. β-actin was used as a loading control. The Bax/Bcl-2 ratio was normalized to β-actin and quantified using GelQuant software (right panels).

To understand if RCFE had any effect on the metastatic properties, its effect on the migration of these cells were studied. HT-29 and A549 cells were treated with 0.05 and 0.1 µg/ml RCFE for 24 and 48 hr **(Fig 4.13.A and 4.13.B)**. The inhibition of migration

in HT-29 was not significant while about 25% inhibition was found against A549 cells treated with either concentration of RCFE for 24 and 48 hr **(Fig 4.13.C and 4.13.D)**.

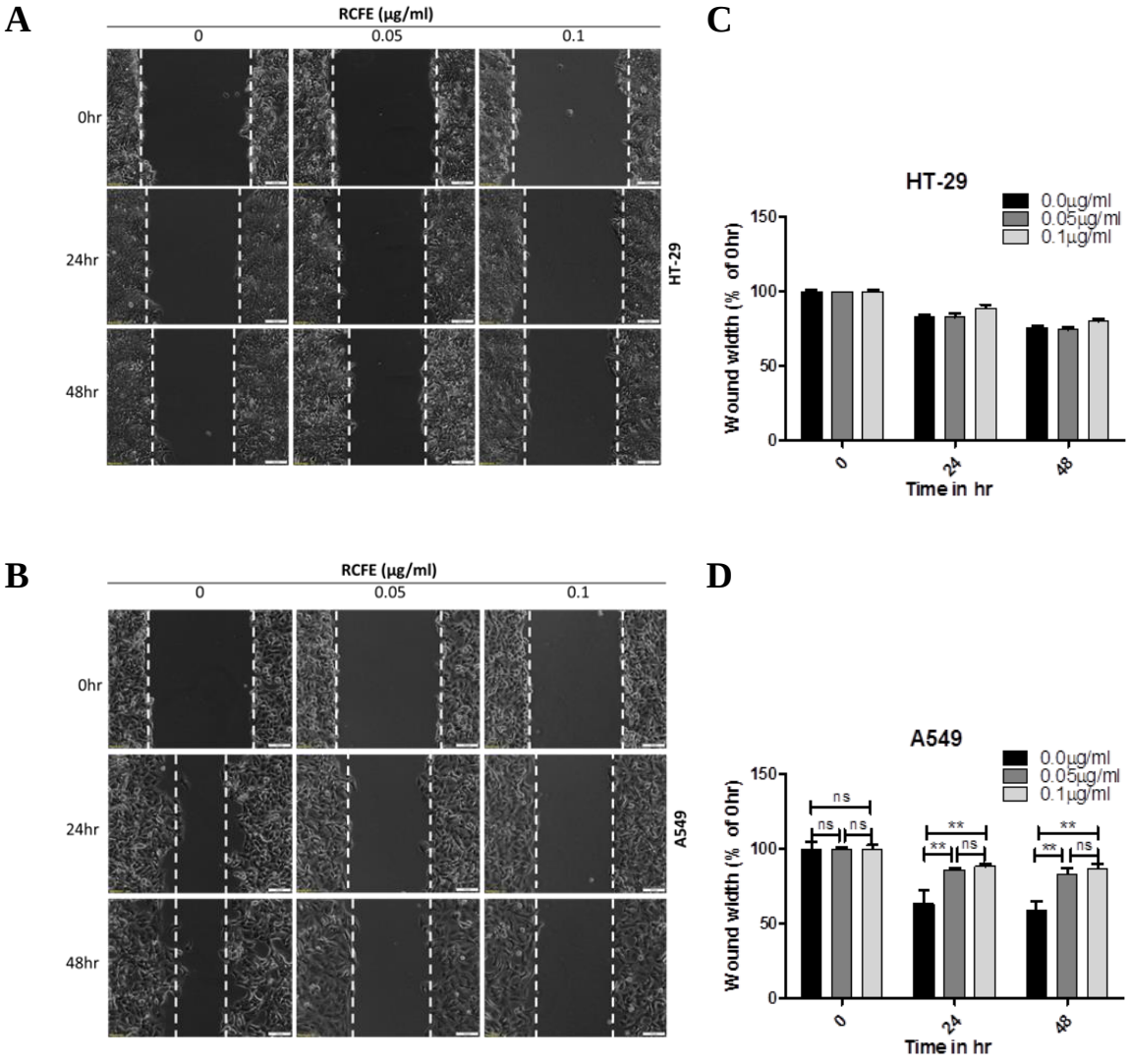

Figure 4.13.: RCFE inhibited the metastatic properties of A549 lung cancer cells. For cell migration using wound healing assay, HT-29 **(A)** and A549 **(B)** were treated with 0.05 and 0.1 µg/ml for 24 and 48 hr. The quantification of wound width as shown in the right panels **(C & D)**. Data represent the mean ± SEM of three independent experiments. Statistical differences were analyzed with a two-way ANOVA test. p-value ns>0.05, p-value ***<0.0001.

4.4.9. Successive fractionation of RCFE and identification of bioactive compounds

As described in the methods section, RCFE was fractionated successively into three fractions RC(E), RC(B) and RC(A). These fractions were subjected to MTT assay for measuring their cytotoxic activity against MCF-7 and MDA-MB-231 cells following their treatment for 24 and 48 hr **(Fig 4.14.A-D)**. The results suggest that among all the

three fractions of RCFE, the ethyl acetate fraction RC(E) showed highest inhibition in both the cell lines. This indicated that the active ingredients of RCFE which impart the anti-cancer effect could be present in the RC(E) fraction.

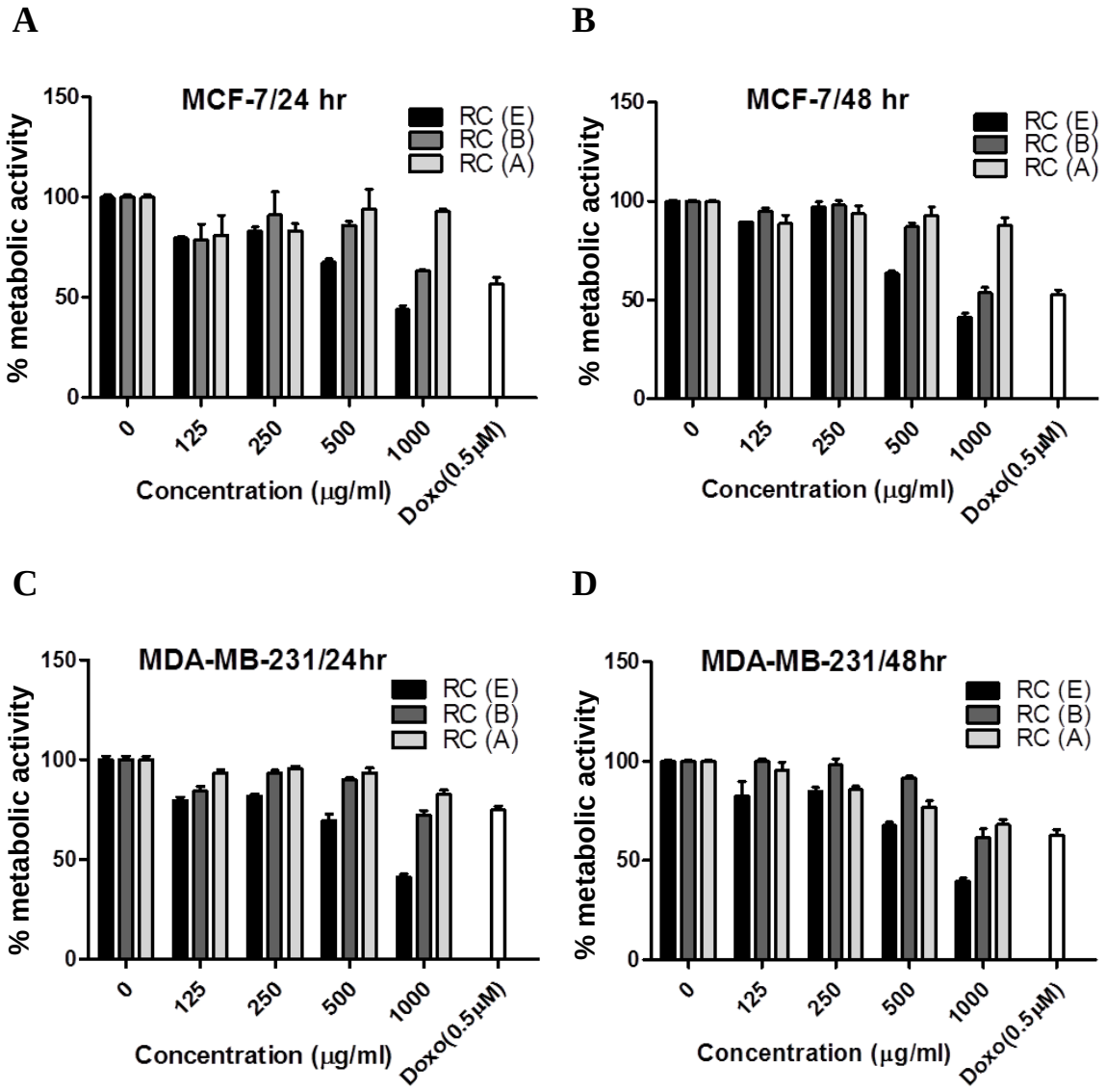

Figure 4.14.: Cytotoxic effect of various fractions of RCFE on human breast cancer cells. Cytotoxic effect on MCF-7 and MDA-MB-231 cells were studied after treatment with three different fractions RC(E) (Ethyl acetate fraction), RC(B) (n-Butanol fraction) and RC(A) (Aqueous fraction) of RCFE for 24 and 48 hr. Doxorubicin (Doxo) has been used as a positive control. Figure **(A)** and **(B)** represented data of MCF-7 and figure **(C)** and **(D)** represented data of MDA-MB-231 after treatment with each fraction for 24 and 48 hr, respectively. Data represent the mean ± SEM of three independent experiments.

Next, to identify the active compounds in RC(E) the fraction was subjected to HPLC fingerprinting analysis. Four characteristic peaks were identified in the RP-HPLC analysis at retention times of 6.36, 10.87, 32.64, 34.80 min **(Fig 4.15.A & 4.15.B)**. The major peaks eluted after HPLC were collected, evaporated and further their ESI-MS

was recorded **(Fig 4.16.A-D)** against commercially available standards. The probable compounds peaks were recognized as Ricinine [26], p-Coumaric acid [27], Epigallocatechin [28] and Ricinoleic acid [27] by comparing ESI-MS spectra with the standards as well as previously reported literature. Retention time, name, molecular formula, molecular weight and chemical structure of the components are shown in **Table 1**.

A

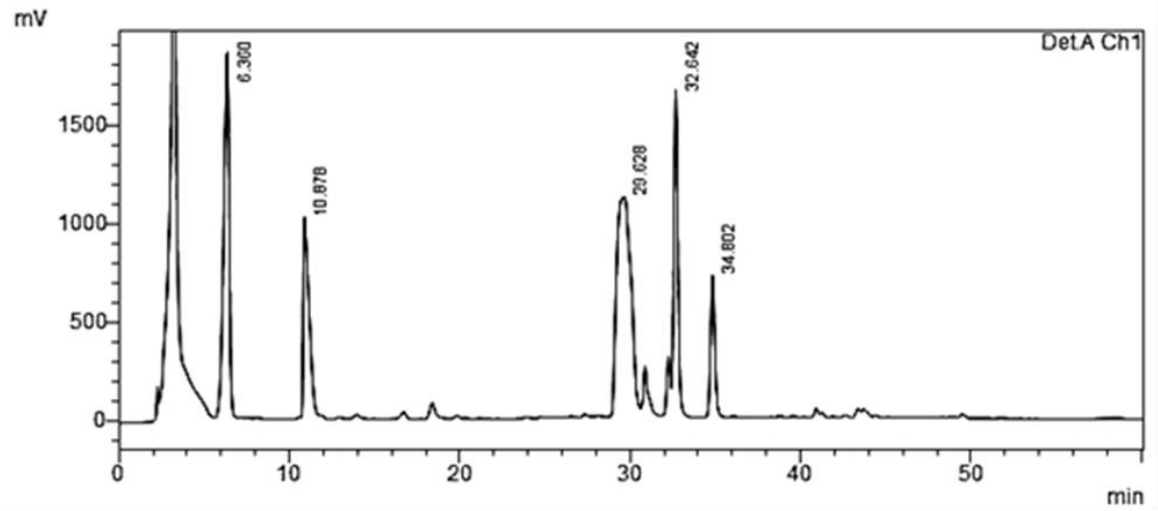

B

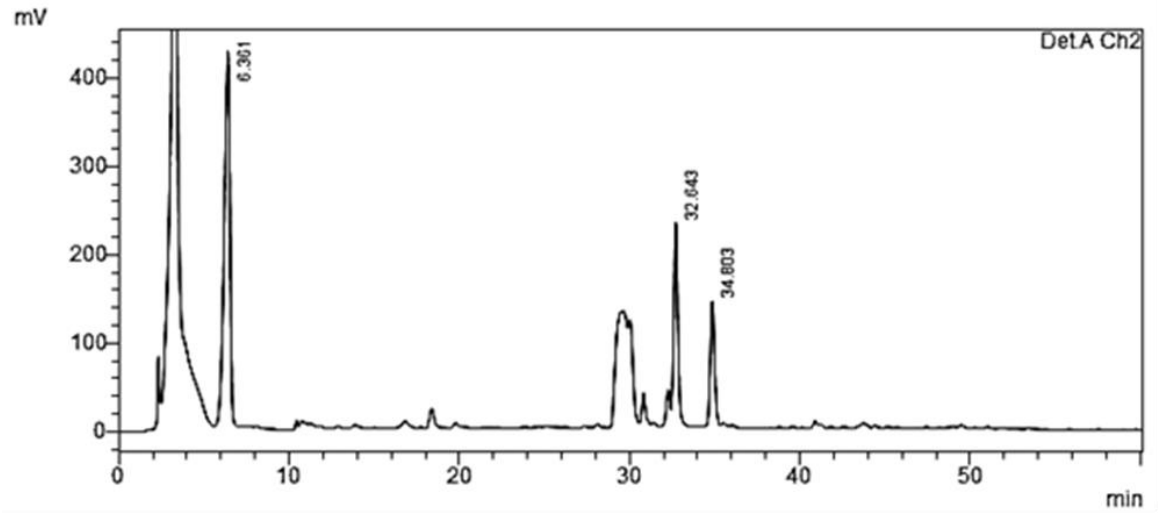

Figure 4.15.: HPLC chromatogram of an ethyl-acetate fraction of RCFE. The chromatogram obtained by running the fraction in a gradient of water: acetonitrile::0.90:0.10 at a flow rate of 1 ml/min and detected at a wavelength of **(A)** 210 nm (Det A Ch1) and **(B)** 254 nm (Det B Ch2).

A

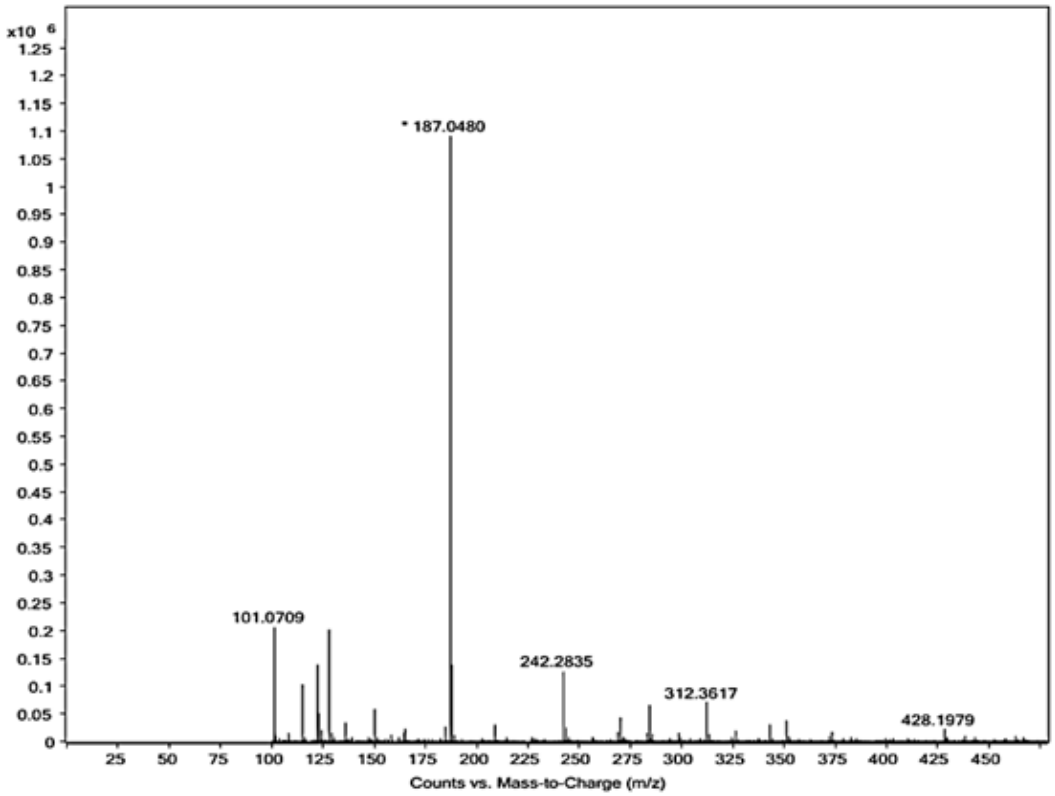
x10 6
* 187.0480
101.0709
242.2835
312.3617
428.1979
Counts vs. Mass-to-Charge (m/z)

B

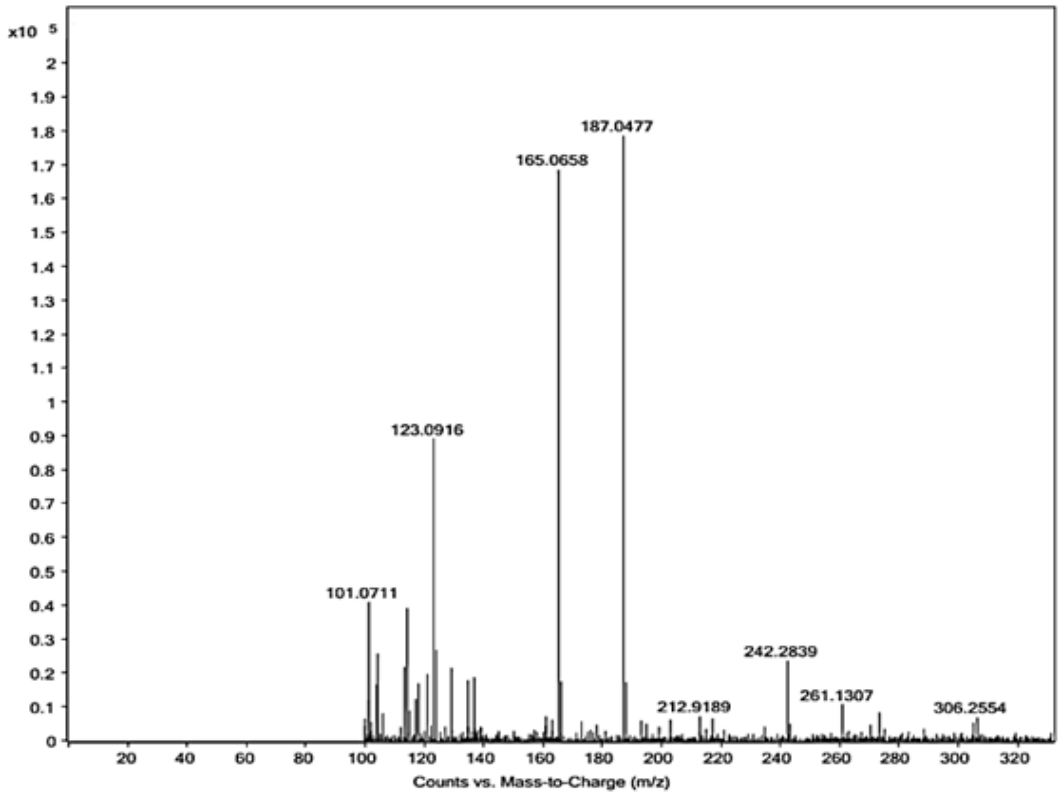
x10 5
187.0477
165.0658
123.0916
101.0711
242.2839
261.1307
212.9189
306.2554
Counts vs. Mass-to-Charge (m/z)

C

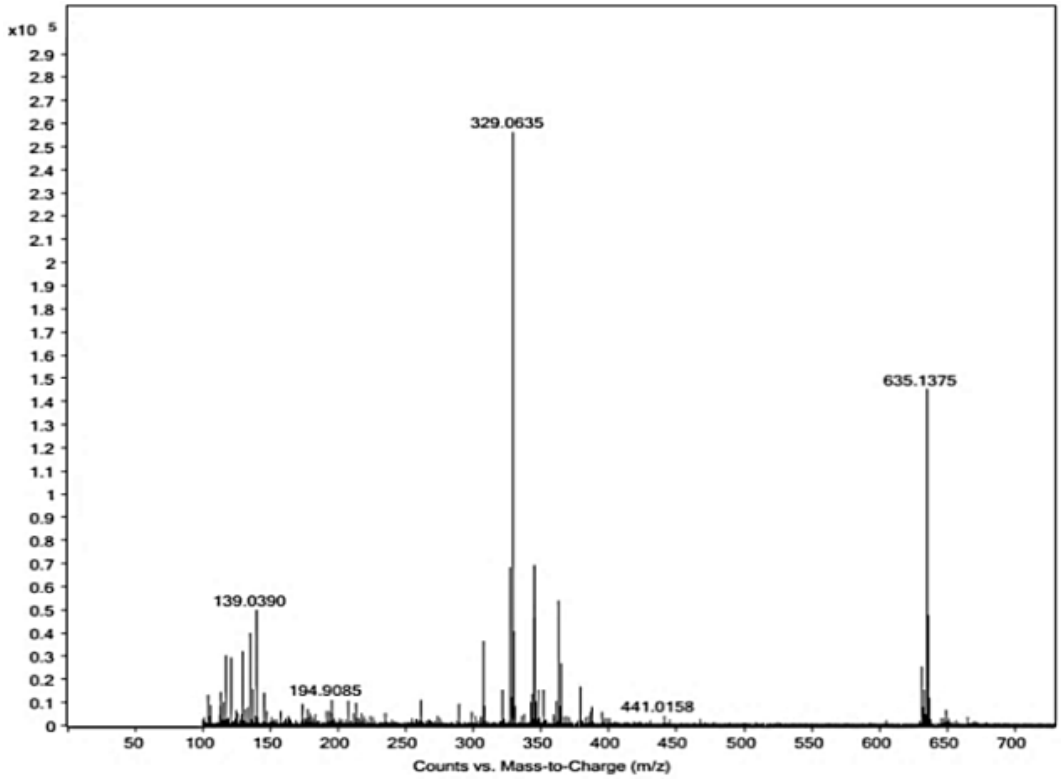

D

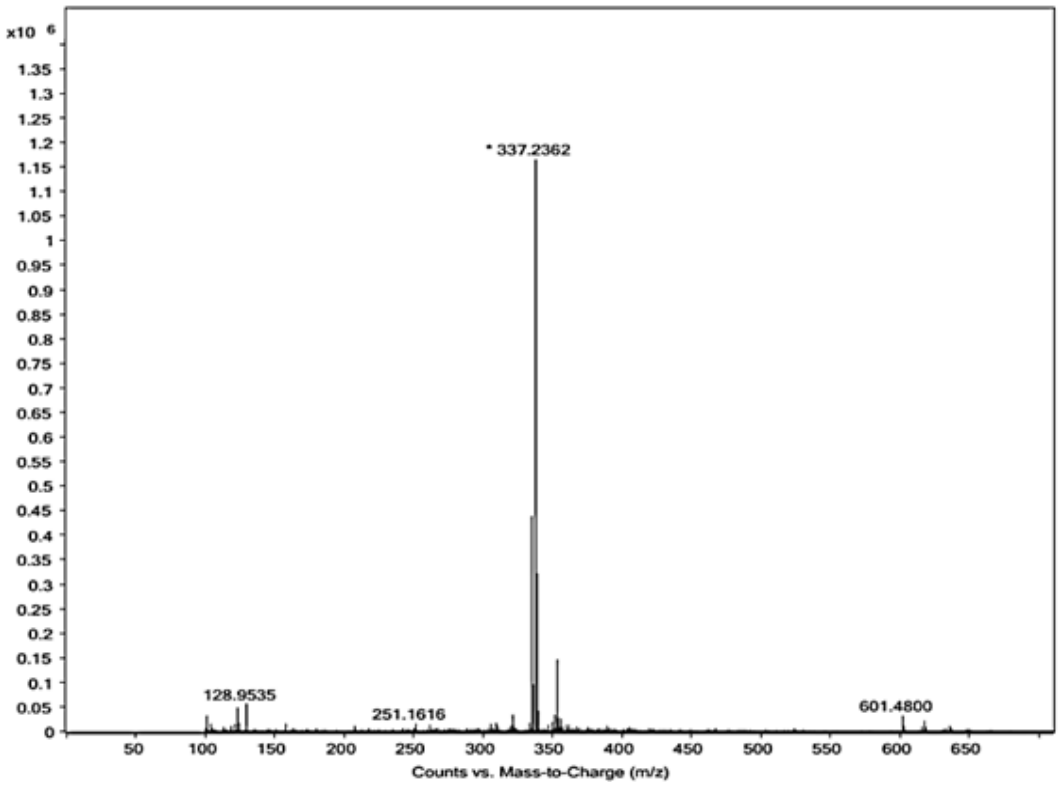

Figure 4.16.: ESI-MS spectra of Ricinine **(A)**, p-Coumaric acid **(B)**, Epigallocatechin **(C)** and Ricinoleic acid **(D)**.

Table 4.1.: Probable compounds identified by HPLC and ESI-MS technique in RCFE

Sl No.	t_R (min)	Comparative area %	m/z (M^+)	m/z (M+Na)	m/z (M+K)	Molecular formula	Compound name & structure	References
1	6.36	26.015	164	187.04	-	$C_8H_8N_2O_2$	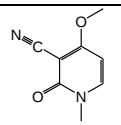 Ricinine	[26]
2	10.87	14.387	164	187.04	-	$C_9H_8O_3$	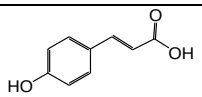 p Coumaric Acid	[27]
3	32.64	14.499	306	329.06	-	$C_{15}H_{14}O_7$	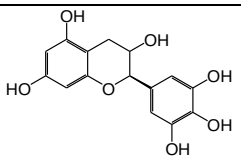 Epigallocatechin	[28]
4	34.80	7.661	298	-	337.23	$C_{18}H_{34}O_3$	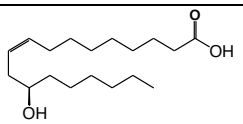 Ricinoleic Acid	[27]

4.4.10. The anticancer activity of pure compounds

To evaluate the cytotoxicity of four compounds identified from RC(E), MCF-7 and MDA-MB-231 cell lines were treated with increasing concentrations of the Ricinine, p-Courmaric acid, Epigallocatechin and Ricinoleic acid for 24 hr. All four compounds showed cytotoxicity against both the cells in a dose-dependent manner **(Fig 4.17.A)**. However, our data suggested that Ricinine, p-Coumaric acid and Ricinoleic acid were comparatively more effective against MDA-MB-231 cells and Epigallocatechin was more effective against MCF-7. All four compounds were found effective in the concentration 50 µM and more. Doxorubicin 0.5µM was used as a positive control in the experiment.

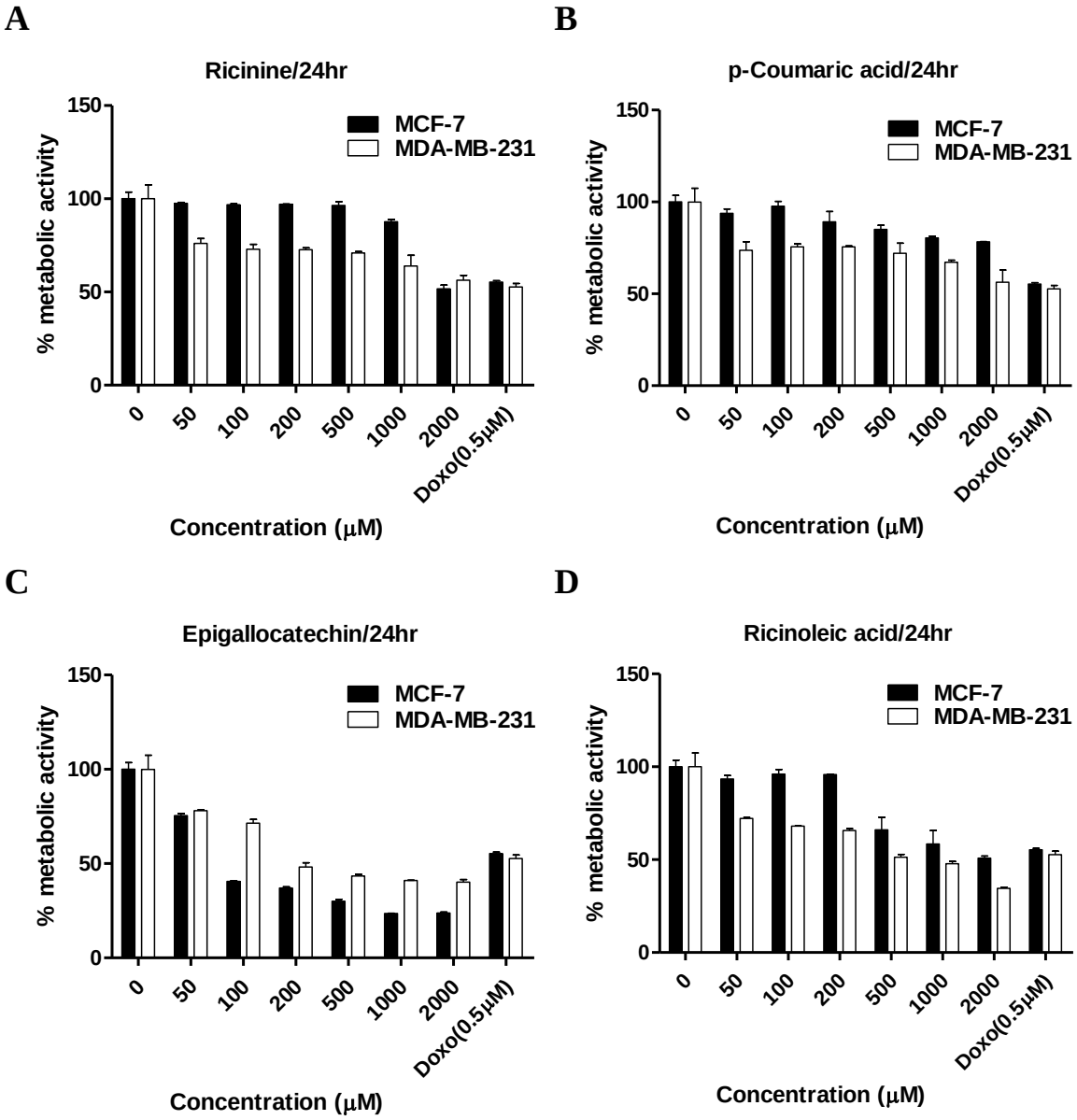

Figure 4.17.: Pure compounds showed a cytotoxic effect in MCF-7 and MDA-MB-231 cells. Percentage of viable MCF-7 and MDA-MB-231 cells after 24 hr of Ricinine **(A)**, p-Coumaric acid **(B)**, Epigallocatechin **(C)**, and Ricinoleic acid **(D)** treatment. Doxorubicin (0.5 μM) was used as a positive control. Data represented the mean ± SD of three independent experiments.

The effect of the four pure compounds on the migration of MCF-7 and MDA-MB-231 cells was studied after 24 and 48 hr incubation with the individual compounds using wound healing assay **(Fig 4.18.A & 4.19.A)**. The inhibition of MCF-7 cell migration was not significant for the compounds after 24 hr of treatment with two concentrations of 10 and 20 μM. However, the effect was more prominent after 48 hr of treatment which showed inhibition of MCF-7 migration by Ricinine, Epigallocatechin, and Ricinoleic acid **(Fig 4.18.B-E)**. The scenario was different in MDA-MB-231 cells where Ricinine and p-Coumaric acid showed no effect after 24 hr treatment and

moderate effect after 48 hr **(Fig 4.19.B-E)**. Interestingly, Epigallocatechin treatment strongly inhibited MDA-MB-231 cell migration in a dose and time-dependent manner **(Fig 4.19.C)**. The inhibitory effect of Ricinoleic acid on the migration of MDA-MB-231 cells was also highly significant after 48 hr of treatment.

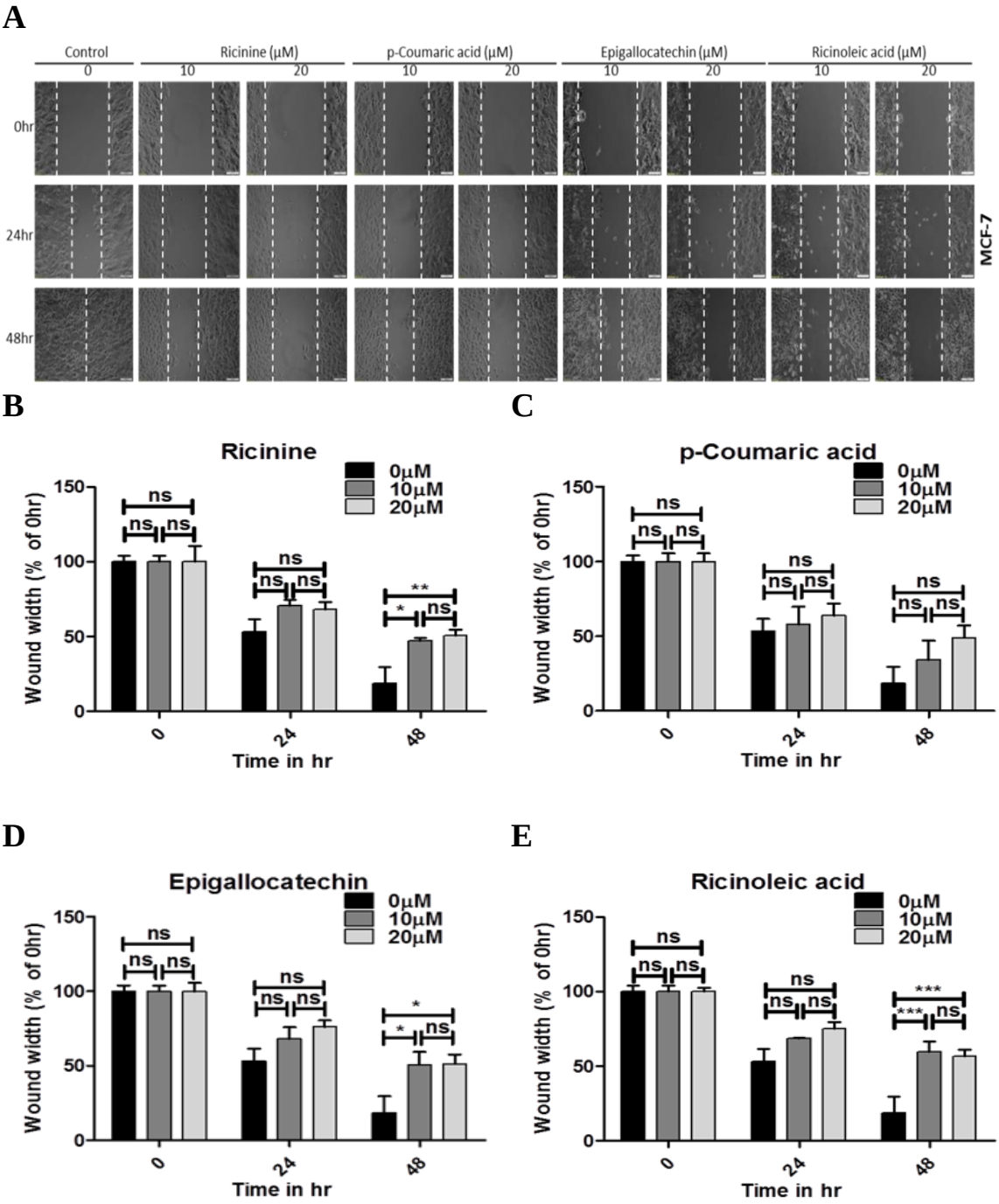

Figure 4.18.: Pure compounds showed migration inhibitory effect in MCF-7 cells. Inhibition of migration of MCF-7 **(A)** with the treatment of 10 and 20 µM for 24 and 48 hr. Percentage of wound width in the cells after Ricinine **(B)**, p-Coumaric acid **(C)**, Epigallocatechin **(D)**, and Ricinoleic acid **(E)** treatment. Data represented the mean ± SD of three independent experiments. Statistical differences were analyzed with a two-way ANOVA test for wound healing assay. p-value >0.05 was considered non-significant (ns) and p-value <0.05 (***<0.0001;**<0.001and **<0.01) was considered significant.

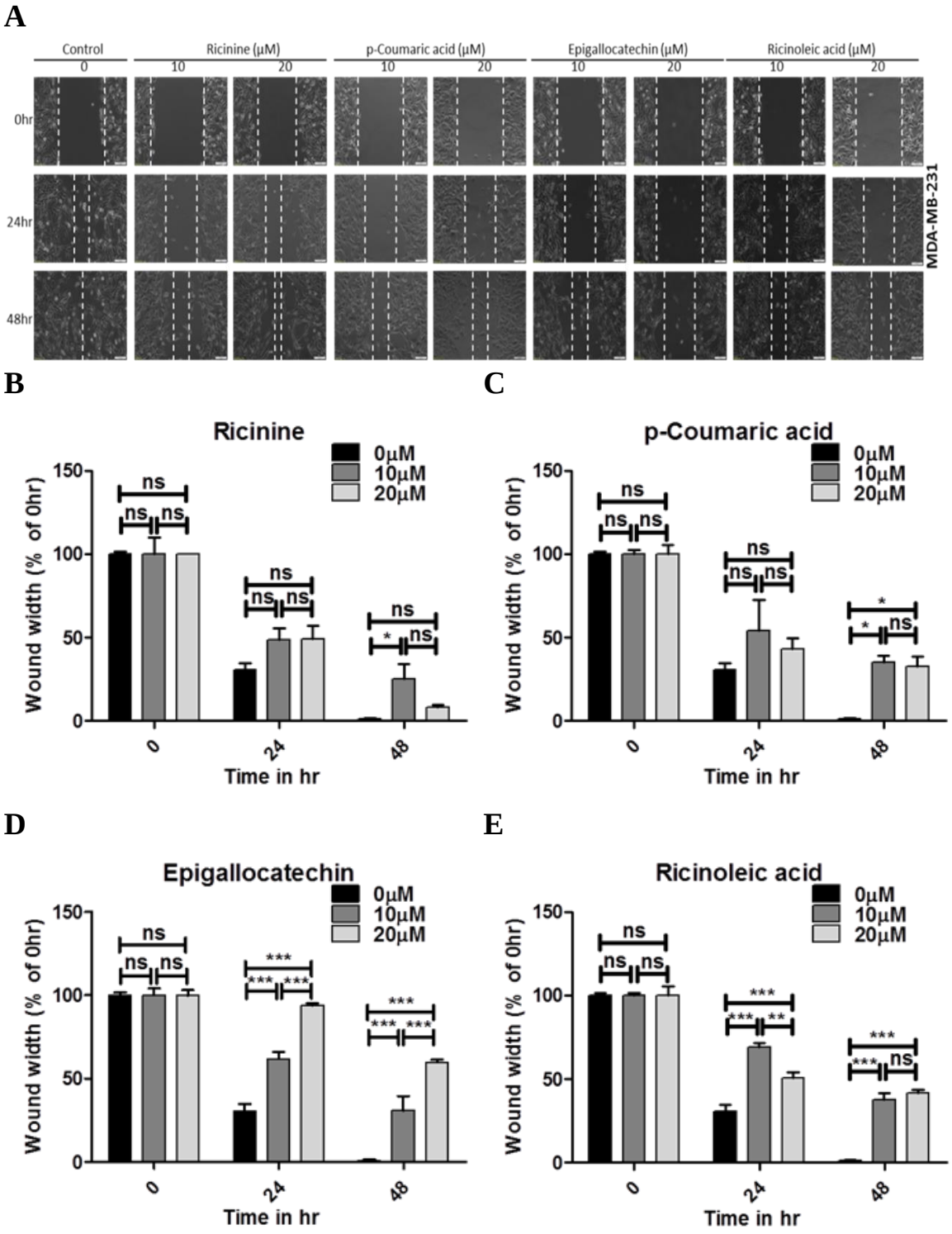

Figure 4.19.: Pure compounds showed a migration inhibitory effect in MDA-MB-231 cells. Inhibition of migration of MDA-MB-231 **(A)** with treatment of 10 and 20 µM for 24 and 48 hr. Percentage of wound width in the cells Ricinine **(B)**, p-Coumaric acid **(C)**, Epigallocatechin **(D)**, and Ricinoleic acid **(E)** treatment. Data represented the mean ± SD of three independent experiments. Statistical differences were analyzed with a two-way ANOVA test for wound healing assay. p-value >0.05 was considered non-significant (ns) and p-value <0.05 (***<0.0001;**<0.001and **<0.01) was considered significant.

The effect of the pure compounds on the adhesion of MCF-7 and MDA-MB-231 cells was also studied. Pre-treatment of both the cells with two non-toxic concentrations (10 and 20 µM) of the individual compounds demonstrated a significant reduction in the adhesion of the cells to collagen IV coated wells in a dose-dependent fashion except in MCF-7 cells treated with p-coumaric acid which shows increase in adhesion efficiency **(Fig 4.20.A and 4.20.B)**. Overall the extent of significance was more in MDA-MB-231 cells as compared to in MCF-7 cells.

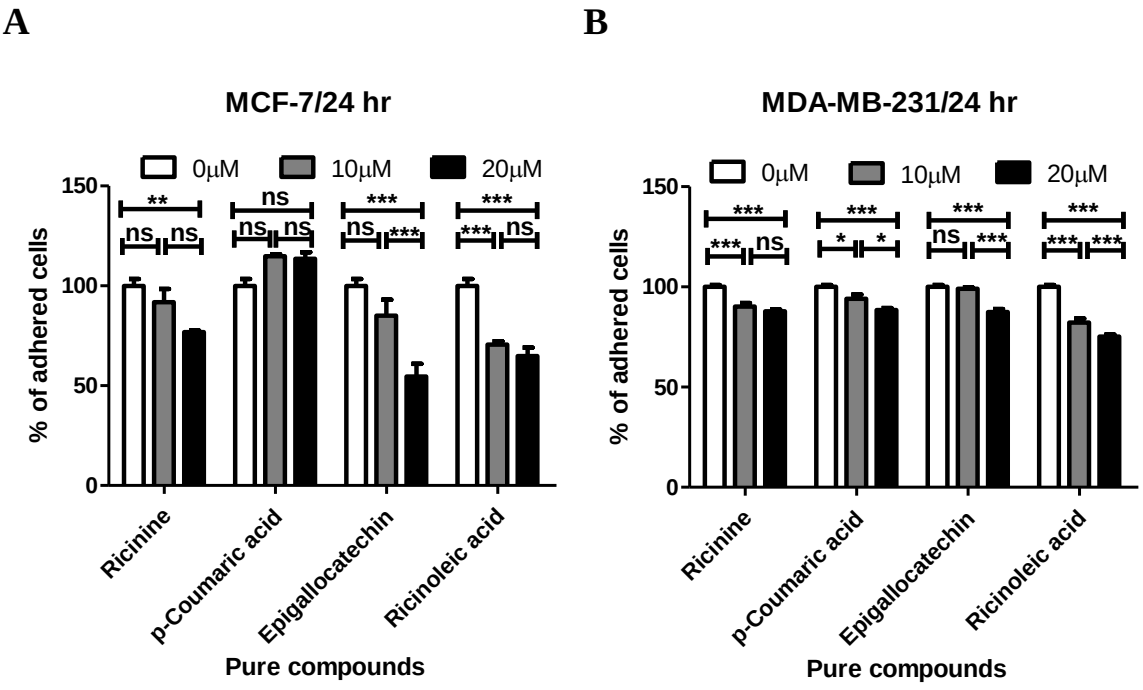

Figure 4.20.: Pure compounds affect the adhesion of MCF-7 and MDA-MB-231 cells. Percentage of MCF-7 **(A)** and MDA-MB-231 **(B)** cells after 24 hr treatment with Ricinine, p-Coumaric acid, Epigallocatechin, and Ricinoleic acid. Data represented the mean ± SD of three independent experiments. Statistical differences were analyzed with a two-way ANOVA test for wound healing assay. p-value >0.05 was considered non-significant (ns) and p-value <0.05 (***<0.0001;**<0.001and **<0.01) was considered significant.

4.5. Discussion

It is now well documented that medicinal plants are a 'treasure trove' of bioactive molecules for the treatment of various human diseases. In the last few decades, numerous traditional knowledge-based drugs have been isolated and commercialized [29-32]. Multiple molecules of medicinal plant origin are currently used as drugs to combat cancer (e.g. vincristine, vinblastine, taxol, paclitaxel, Podophyllotoxin) [3,33-

35]. The current study reports the mechanistic details of anti-cancer activities of the fruit extract of *Ricinus communis* L. (RCFE), commonly known as the castor bean plant. Oil and seeds of this plant are widely used in folk medicine as purgative, against worm infestation and arthritis [36-39]. It has also been reported to have anti-inflammatory effects [40,41]. However, there are no detailed reports on the mechanism of the anti-cancer efficacy of this plant.

Metastasis, the property that empowers certain cancer cells to spread into local or distant tissues is a complex process involving migration, adhesion, and invasion [42,43]. These processes can be targeted by an anti-metastatic agent leading to the attenuated aggression of cancer cells [44]. The migration of cancer cells to different tissues is an important initial step in metastasis [45,46]. Treatment with RCFE inhibited migration of both MCF-7 and MDA-MB-231 in a dose-dependent manner. The initiation of metastasis also depends on adhesion property of the cells that involves interaction with the extracellular matrix following detachment from the primary sites [47,48]. RCFE at very low concentrations significantly inhibited adhesion of cells with collagen IV which is an integral part of the basement membrane [49]. The process of invasion is critical for metastasis because the motile cells need to cross the extracellular matrix and spread into surrounding tissues [50]. In this study, RCFE substantially inhibited the efficacy of the cells to invade ECM gel to reach another side of the insert in response to a media containing 10% FBS. The highest inhibition of invasion (81%) was achieved in MDA-MB-231 cells after treatment with a very low concentration of 0.1 µg/ml of RCFE for 24 hr. Remarkably, RCFE showed greater inhibition of cell migration and invasion in highly aggressive triple-negative MDA-MB-231 cells compared to MCF-7 cells suggesting its probable application to manage highly aggressive cancer cells. The process of invasion and metastasis is accompanied by degradation of connective tissues and as a result expression of matrix-degrading enzymes e.g. matrix metalloproteinases (MMPs) increases [51-55]. MMP-2 and 9 have been shown to overexpress and contribute to metastatic efficacy of MDA-MB-231 [56]. Here, we showed that the expression of MMP-2 and 9 was inhibited by RCFE emphasizing its effect on ECM degradation and invasion of cancer cells.

Apoptosis is a key mechanism for cell death which leads to fragmettation of DNA in cells [57-59]. DNA fragmentation assay is a widely used biochemical marker of

apoptosis [60]. DNA fragmentation occurs at the inter-nucleosomal linker regions in the cells undergoing apoptosis that can be visualized as a ladder like smear when run in agarose gel [61-63]. [64]. Genomic DNA isolated from the cells following treatment of RCFE (1µg/ml) in 24 and 48 hr demostrated degradation in both cells and indicated the efficacy of RCFE to induce apoptosis in both the cells. Further, Annexin V-FITC/PI microscopic assay also indicated the induction of apoptosis by RCFE in both the cells. Green fluorescence implies early apoptosis in the cells as exposure of membrane phospholipid phosphatidylserine (PS) to the extracellular environment prompts its binding to Annexin V [65]. The red fluorescence is generated by cells that are dead or in the late stage of apoptosis and therefore, their membrane becomes permeable to PI [65]. Treatment of RCFE induced apoptosis to both MCF-7 **(Fig 4.5.B)** and MDA-MB-231 **(Fig 4.5.C)** cells. Quantification of the cell death in these cells via apoptosis was studied using flow cytometry analysis. It was clear from the analysis that, RCFE induced apoptosis in a significant percentage of cells **(Fig 4.6)**. To elucidate the mechanism of apoptosis, expression of several pro and anti-apoptotic proteins were studied by western blot. RCFE inhibited the expression of anti-apoptotic protein Bcl-2 and induced the expression of pro-apoptotic protein Bax. Expression of Bcl-2 and Bax family proteins plays a significant role in inducing apoptosis in a cell by altering the release of cytochrome c from mitochondria as a result of increased mitochondrial membrane permeability [66]. Inhibition of Bcl-2 by RCFE possibly induced cytochrome c production that led to the expression of caspases. Caspases are the key players in apoptosis and a variety of caspases are involved in intrinsic, extrinsic and execution pathways of associated to apoptosis [66]. Caspases utulize PARP as substrate leading to its cleavage during apoptosis [66-68]. One of the critical caspase family members involved in execution pathway, Caspase 7, was up-regulated in both MCF-7 **(Fig 4.7.A)** and MDA-MB-231 **(Fig 4.7.B)** confirming its role in inducing apoptosis in response to RCFE. Further, increased PARP cleavage with the treatment of increasing concentration of RCFE supported this observation. Expression of p53, a key regulator of apoptosis and cell cycle arrest, did not increase suggesting its minimal role in inducing apoptosis following RCFE treatment [69,70]. p53 regulates the inhibitory signals/proteins for cell cycle progression and act as a master regulator for both G1/S phase as well as G2/M phase progression. Cyclins are required by CDKs for cell cycle progression [71-73]. Hence, the level of Cyclin E1 protein after RCFE treatment was studied which remained

almost unchanged in both the cell lines suggesting that cell cycle was not probably arrested by RCFE. Further, to understand the specificity, RCFE was studied for its activity against four additional cencer cell lines, two from breast origin (HER2 +ve MDA-MB-453 and triple +ve ZR-75-1), one from colon origin (HT29) and another from lung origin (A549). RCFE showed promising cototoxic activity in these cell lines suggesting the extract could be used in various types of cancer cells (**Fig 4.10.A-D).** In fact, further studies on the expression apoptosis associated proteins suggested apoptosis could be induced in HT29 and A549 cell by RCFE **(Fig 4.11.)**. Migration assay was performed in these cells and the extract was highly effective in regulating migration of A549; however, the inhibition was not significant in HT29 (**Fig 4.12**). Interestingly, no significant cytotoxicity was induced by RCFE in HEK293 and mouse embryonic fibroblast (MEF) at a concentration of 1.0 µg/ml (shown in **Fig 3.3**). However, treatment with this concentration induced significant cytotoxicity in all the six experimental cancer cell lines. It would be tempting to hypothesize that RCFE induce cytotoxicity specifically in cancer cells, however, additional studies should be performed before we come to a conclusion.

The differential regulation by RCFE involving prevention of metastatic activity and induction of apoptosis might be attributed to its activity to down-regulate phosphorylation of STAT3, a master regulator for these two pathways in cancer cells [74-76]. Unusual JAK-STAT signaling (specifically STAT3) is common in various cancer due to their constitutive activation in response to stimulators e.g. cytokines, growth factors, receptors (TLRs/ GPCRs), polypeptide ligands and miRNAs [77]. STAT3 induces expression of MMPs and promotes invasion and metastasis in cancer cells [76]. In addition, it induces anti-apoptotic Bcl-2 expression leading to the survival of the cells. So, targeting STAT3 was suggested as a viable therapeutic strategy against cancer [77]. RCFE mediated deactivation of Tyr705 phosphorylation of STAT3 inhibited these two critical steps leading to attenuation of metastatic and induction of apoptosis suggesting a possible application of this extract against breast cancer therapy.

The anti-cancer efficacy of RCFE was highlighted by the 4T1 syngeneic mouse model [78,79]. 4T1 cells are highly tumorigenic and thus suitable for the generation of mammary tumors in animals with characters close to human mammary tumors [79,80]. Our data suggested that 4 doses of intraperitoneal administrations of RCFE at a

concentration as low as 0.5 mg/kg body weight reduced the tumor volume by about 88% emphasizing its role in limiting breast tumors *in vivo.* Several animal models are reported to study the efficacy of drugs against breast cancer: xenograft, genetically engineered (transgenic) and syngeneic models being the most common of them. While xenograft models are popular as it mimics human tumors, it eliminates the possibility of the immune response against the tumor leading to host-tumor interaction unnatural to human tumor development [81]. Transgenic animal models overcome this problem and can be used to screen drugs against tumorigenesis. However, genetic changes should be tissue-specific in these models, as oncogene-bearing or tumor suppressor gene-knockout systemically may not imitate tumors arising out of mutations in normal microenvironment [81]. These models also take several months to generate tumor and are expensive. Syngeneic models, on contrary, are simple and inexpensive models. Murine adenocarcinoma 4T1 cells implanted in immunocompetent Balb/c, as demonstrated in this study, is the most widely used syngeneic model to study tumor progression and metastasis [82].

It is important to have knowledge about constituent molecule(s) of a bioactive plant extract for its probable use as therapy. We performed HPLC and ESI-MS analysis of the ethyl acetate fraction of the extract which revealed the presence of four individual compounds namely, Ricinine, p-Coumaric acid, Epigallocatechin, and Ricinoleic Acid. Of them, Ricinine and Ricinoleic Acid have not been reported for any anti-cancer activity albeit their prominent pharmacological importance [83-85]. However, p-Coumaric acid, a hydroxy derivative of cinnamic acid was shown to inhibit the proliferation of colon cancer cells in a dose-dependent manner [86]. It induced apoptosis accompanied by increasing reactive oxygen species (ROS) levels, a fall in the mitochondrial membrane potential and increased lipid layer breaks. Ethanolic extract of Chinese propolis, where p-Coumaric acid is one of the components, exerts antitumor effects mainly through inducing apoptosis of breast cancer cells [87]. Furthermore, Epigallocatechin was also reported for inducing apoptosis and cell cycle arrest [88]. We studied the cytotoxic and migration-inhibitory efficacy of all four compounds to have insight into their individual roles as anti-cancer molecules. Though all four compounds showed cytotoxicity, their efficacy varied with cell types. The inhibition of migration of in MCF-7 cells **(Fig 4.18.)** was possibly due to a combination of Ricinine, Epigallocatechin and Ricinoleic acid as an effect of p-coumaric acid were found to be

nominal. Interestingly, in highly metastatic MDA-MB-231 cells, Epigallocatechin contributed most significantly to abrogating migration. However, Ricinoleic acid and Ricinine also contributed moderately to inhibit migration in MDA-MB-231 cells **(Fig 4.19.)**. These four compounds are also effective in inhibiting adhesion of the two cell lines individually up to different extends. The effect of Epigallocatechin on MCF-7 cells is the best among all **(Fig 4.20.)**.

In summary, our study demonstrated the efficacy of the fruit extract of common castor plant *R. communis* L. against two breast cancer cells of distinctive characteristics. The extract inhibited the aggressiveness of the cancer cells by inhibiting characters of metastasis such as cell motility, adhesion, invasion, and reduced MMP-2 and 9 expressions. Treatment with the extract induced apoptosis in the cells by augmenting the Bax/Bcl-2 ratio that is known to induce caspases and subsequent cleavage of PARP. The phosphorylation of STAT3, a central regulator for activation of metastasis and anti-apoptotic molecules, was inhibited by the extract. The extract significantly reduced tumor volumes in 4T1 syngeneic mouse model. HPLC fingerprinting along with ESI-MS analysis suggested the presence of four compounds, all of which showed anti-cancer efficacy individually. This study contributes to the repertoire of plant-derived therapeutic strategies for the treatment of breast cancer.

4.6. Bibliography

[1] Roy, A., Jauhari, N., and Bharadvaja, N. Medicinal plants as. *Anticancer Plants: Natural Products and Biotechnological Implements*, 2: 109,

[2] Balunas, M. J. and Kinghorn, A. D. Drug discovery from medicinal plants. *Life sciences*, 78(5): 431-441, 2005.

[3] Cragg, G. M. and Newman, D. J. Plants as a source of anti-cancer agents. *Journal of ethnopharmacology*, 100(1-2): 72-79, 2005.

[4] Greenwell, M. and Rahman, P. Medicinal plants: their use in anticancer treatment. *International journal of pharmaceutical sciences and research*, 6(10): 4103, 2015.

[5] Pezzuto, J. M. Plant-derived anticancer agents. *Biochemical pharmacology*, 53(2): 121-133, 1997.

[6] Shah, U., Shah, R., Acharya, S., and Acharya, N. Novel anticancer agents from plant sources. *Chinese journal of natural medicines*, 11(1): 16-23, 2013.

[7] Kaur, R., Kapoor, K., and Kaur, H. Plants as a source of anticancer agents. *J Nat Prod Plant Resour*, 1(1): 119-124, 2011.

[8] Darmanin, S., Wismayer, P. S., Camilleri Podesta, M. T., Micallef, M. J., and Buhagiar, J. A. An extract from Ricinus communis L. leaves possesses cytotoxic properties and induces apoptosis in SK-MEL-28 human melanoma cells. *Nat Prod Res*, 23(6): 561-571, 2009. 10.1080/14786410802228579

[9] Sani, U. and Sule, M. Anti-fertility activity of methanol extracts of three different seed varieties of Ricinus communis Linn (Euphorbiaceae). *Nigerian Journal of Pharmaceutical Sciences*, 6(2): 78-83, 2007.

[10] Prakash, E. and D.K.Gupta. In Vitro Study of Extracts of Ricinus communis Linn on Human Cancer Cell lines. *Journal of Medical Sciences and Public Health*, 2(4): 15-20, 2014.

[11] JENA, J. and GUPTA, A. K. *Ricinus communis* Linn: a phytopharmacological review. *International Journal of Pharmacy and Pharmaceutical Sciences*, 4(4): 25-29, 2012.

[12] Visen, P., Shukla, B., Patnaik, G., Tripathi, S., Kulshreshtha, D., Srimal, R., and Dhawan, B. Hepatoprotective activity of Ricinus communis leaves. *International journal of pharmacognosy*, 30(4): 241-250, 1992.

[13] Shokeen, P., Anand, P., Murali, Y. K., and Tandon, V. Antidiabetic activity of 50% ethanolic extract of Ricinus communis and its purified fractions. *Food and Chemical Toxicology*, 46: 3458–3466, 2008. 10.1016/j.fct.2008.08.020

[14] Sandhyakumary, K., Bobby, R., and Indira, M. Antifertility effects of Ricinus communis (Linn) on rats. *Phytotherapy Research*, 17(5): 508-511, 2003.

[15] Ilavarasan, R., Mallika, M., and Venkataraman, S. Anti-inflammatory and free radical scavenging activity of Ricinus communis root extract. *Journal of ethnopharmacology*, 103(3): 478-480, 2006.

[16] Gargade and D.G, K. Screening of antibacterial activity ofRicinus communisL. leaves extracts against Xanthomonas axonopodis pv. punicae. *International Journal of Advanced Research in Biological Sciences*, 2(9): 47-51, 2015.

[17] Sitton, D. and West, C. A. Casbene: An anti-fungal diterpene produced in cell-free extract's of ricznus communis seedlings. *Phytochemistry*, 14: 1921-1925, 1957.

[18] Upasani, S. M., Kotkar, H. M., Mendki, P. S., and Maheshwari∗, V. L. Partial characterization and insecticidalproperties of Ricinus communis Lfoliage flavonoids. *Pest Management Science*, 599: 1349–1354, 2003. 10.1002/ps.767

[19] Rodriguez, L. G., Wu, X., and Guan, J.-L. Wound-healing assay. In, *Cell Migration*, of, pages 23-29. Springer, 2005.

[20] Yarrow, J. C., Perlman, Z. E., Westwood, N. J., and Mitchison, T. J. A high-throughput cell migration assay using scratch wound healing, a comparison of image-based readout methods. *BMC biotechnology*, 4(1): 21, 2004.

[21] Chen, Y. Cell adhesion assay. *Bio-protocol*, 1: e98, 2011.

[22] Marshall, J. Transwell® invasion assays. In, *Cell Migration*, of, pages 97-110. Springer, 2011.

[23] Kramer, N., Walzl, A., Unger, C., Rosner, M., Krupitza, G., Hengstschläger, M., and Dolznig, H. In vitro cell migration and invasion assays. *Mutation Research/Reviews in Mutation Research*, 752(1): 10-24, 2013.

[24] Loo, D. T. In situ detection of apoptosis by the TUNEL assay: an overview of techniques. In, *DNA Damage Detection In Situ, Ex Vivo, and In Vivo*, of, pages 3-13. Springer, 2011.

[25] Attardi, L. D., de Vries, A., and Jacks, T. Activation of the p53-dependent G1 checkpoint response in mouse embryo fibroblasts depends on the specific DNA damage inducer. *Oncogene*, 23(4): 973-980, 2004.

[26] Wachira, S. W., Omar, S., Jacob, J. W., Wahome, M., Alborn, H. T., Spring, D. R., Masiga, D. K., and Torto, B. Toxicity of six plant extracts and two pyridone alkaloids from Ricinus communis against the malaria vector Anopheles gambiae. *Parasites & vectors*, 7(1): 312, 2014.

[27] Wafa, G., Amadou, D., and Larbi, K. M. Larvicidal activity, phytochemical composition, and antioxidant properties of different parts of five populations of Ricinus communis L. *Industrial Crops and Products*, 56: 43-51, 2014.

[28] Singh, P. P. and Chauhan, S. Activity guided isolation of antioxidants from the leaves of Ricinus communis L. *Food chemistry*, 114(3): 1069-1072, 2009.

[29] <art%3A10.1007%2FBF00832010.pdf>.

[30] Young-Won Chin, Marcy J. Balunas , Hee Byung Chai , and Kinghorn, A. D. Drug Discovery From Natural Sources. *The AAPS Journal*, 8(2): E239-E253, 2006.

[31] Gordon M. Cragg, David J. Newman, and Snader, K. M. Natural Products in Drug Discovery and Development. *J. Nat. Prod.*, 60: 52-60, 1997.

[32] Rates, S. M. K. Plants as source of drugs. *Toxicon*, 39: 603–613, 2001.

[33] Bhanot, A., Sharma, R., and Noolvi, M. N. Natural sources as potential anti-cancer agents: A review. *International journal of phytomedicine*, 3(1): 09, 2011.

[34] Rowinsky, E. K. and Donehower, R. C. Paclitaxel (taxol). *New England Journal of Medicine*, 332(15): 1004-1014, 1995.

[35] Wang, H.-K. and Lee, K.-H. Plant-derived anticancer agents and their analogs currently in clinical use or in clinical trials. *BOTANICAL BULLETIN-ACADEMIA SINICA TAIPEI*, 38: 225-236, 1997.

[36] Haider, M. and Zhong, L. Ethno-medicinal uses of plants from district Bahawalpur, Pakistan. *Curr Res J Biol Sci*, 6: 183-190, 2014.

[37] Khan, F. M. Ethno-veterinary medicinal usage of flora of Greater Cholistan desert (Pakistan). *Pakistan Veterinary Journal*, 29(2), 2009.

[38] Rahul, J. An ethnobotanical study of medicinal plants in Taindol village, district Jhansi, Region of Bundelkhand, Uttar Pradesh, India. *Journal of Medicinal Plants*, 1(5), 2013.

[39] Jalali, H., Nejad, A. M., Ebadi, A., and Laey, G. Ethnobotany and folk pharmaceutical properties of major trees or shrubs in northeast of Iran. *Asian Journal of Chemistry*, 21(7): 5632, 2009.

[40] Muthamizh, S. and Ramachandran, V. Medicinal plants of Dharmapuri district of Tamil Nadu used in primary healthcare system. *International journal of Botany Studies*, 3(1): 109-119, 2018.

[41] COIMBATORE, F. S. W. G. O. Journal of Science Unani Medicine.

[42] Poste, G. and Fidler, I. J. The pathogenesis of cancer metastasis. *Nature*, 283(5743): 139, 1980.

[43] Gupta, G. P. and Massagué, J. Cancer metastasis: building a framework. *Cell*, 127(4): 679-695, 2006.

[44] Schroeder, A., Heller, D. A., Winslow, M. M., Dahlman, J. E., Pratt, G. W., Langer, R., Jacks, T., and Anderson, D. G. Treating metastatic cancer with nanotechnology. *Nature Reviews Cancer*, 12(1): 39, 2012.

[45] Bravo-Cordero, J. J., Hodgson, L., and Condeelis, J. Directed cell invasion and migration during metastasis. *Current opinion in cell biology*, 24(2): 277-283, 2012.

[46] Jones, D. H., Nakashima, T., Sanchez, O. H., Kozieradzki, I., Komarova, S. V., Sarosi, I., Morony, S., Rubin, E., Sarao, R., and Hojilla, C. V. Regulation of cancer cell migration and bone metastasis by RANKL. *Nature*, 440(7084): 692, 2006.

[47] Gkretsi, V. and Stylianopoulos, T. Cell adhesion and matrix stiffness: coordinating cancer cell invasion and metastasis. *Frontiers in oncology*, 8: 145, 2018.

[48] Balzer, E. M. and Konstantopoulos, K. Intercellular adhesion: mechanisms for growth and metastasis of epithelial cancers. *Wiley Interdisciplinary Reviews: Systems Biology and Medicine*, 4(2): 171-181, 2012.

[49] Leea, H. S., Seob, E. Y., Kangc, N. E., and Kim, W. K. [6]-Gingerol inhibits metastasis of MDA-MB-231 human breast cancer cells. *Journal of Nutritional Biochemistry*, 19: 313-319, 2008. 10.1016/j.jnutbio.2007.05.008

[50] Krakhmal, N., Zavyalova, M., Denisov, E., Vtorushin, S., and Perelmuter, V. Cancer invasion: patterns and mechanisms. *Acta Naturae (англоязычная версия)*, 7(2 (25)), 2015.

[51] Gialeli, C., Theocharis, A. D., and Karamanos, N. K. Roles of matrix metalloproteinases in cancer progression and their pharmacological targeting. *The FEBS journal*, 278(1): 16-27, 2011.

[52] Luca, M., Huang, S., Gershenwald, J. E., Singh, R. K., Reich, R., and Bar-Eli, M. Expression of interleukin-8 by human melanoma cells up-regulates MMP-2 activity and increases tumor growth and metastasis. *The American journal of pathology*, 151(4): 1105, 1997.

[53] Heppner, K. J., Matrisian, L. M., Jensen, R. A., and Rodgers, W. H. Expression of most matrix metalloproteinase family members in breast cancer represents a tumor-induced host response. *The American journal of pathology*, 149(1): 273, 1996.

[54] Deryugina, E. I. and Quigley, J. P. Matrix metalloproteinases and tumor metastasis. *Cancer and Metastasis Reviews*, 25(1): 9-34, 2006.

[55] Duffy, M. J., Maguire, T. M., Hill, A., McDermott, E., and O'Higgins, N. Metalloproteinases: role in breast carcinogenesis, invasion and metastasis. *Breast cancer research*, 2(4): 252, 2000.

[56] Lee, H. S., Seo, E. Y., Kang, N. E., and Kim, W. K. [6]-Gingerol inhibits metastasis of MDA-MB-231 human breast cancer cells. *The Journal of nutritional biochemistry*, 19(5): 313-319, 2008.

[57] Kerr, J. F., Wyllie, A. H., and Currie, A. R. Apoptosis: a basic biological phenomenon with wideranging implications in tissue kinetics. *British journal of cancer*, 26(4): 239, 1972.

[58] Wyllie, A. H., Kerr, J. R., and Currie, A. Cell death: the significance of apoptosis. In, *International review of cytology*, 68 of, pages 251-306, 0074-7696. Elsevier, 1980.

[59] Elmore, S. Apoptosis: a review of programmed cell death. *Toxicologic Pathology*, 35(4): 495-516, 2007.

[60] Compton, M. M. A biochemical hallmark of apoptosis: internucleosomal degradation of the genome. *Cancer and Metastasis Reviews*, 11(2): 105-119, 1992.

[61] CHOI, Y. H. and YOO, Y. H. Taxol-induced growth arrest and apoptosis is associated with the upregulation of the Cdk inhibitor, p21WAF1/CIP1, in human breast cancer cells. *Oncology reports*, 28: 2163-2169,, 2012. 10.3892/or.2012.2060

[62] Nagata, S. Apoptotic DNA Fragmentation. *Experimental Cell Research*, 256: 12-18, 2000. 10.1006/excr.2000.4834

[63] Leist, M., Single, B., Castoldi, A. F., Kühnle, S., and Nicotera, P. Intracellular Adenosine Triphosphate (ATP) Concentration: A Switch in the Decision Between Apoptosis and Necrosis. *Journal of Experimental Medicine*, 185(5): 1481-1486, 1997.

[64] Gorczyca, W., Gong, J., and Darzynkiewicz, Z. Detection of DNA strand breaks in individual apoptotic cells by the in situ terminal deoxynucleotidyl transferase and nick translation assays. *Cancer research*, 53(8): 1945-1951, 1993.

[65] Vermes, I., Haanen, C., Steffens-Nakken, H., and Reutellingsperger, C. A novel assay for apoptosis flow cytometric detection of phosphatidylserine expression on early apoptotic cells using fluorescein labelled annexin V. *Journal of Immunological Methods*, 184(1): 39-51, 1995.

[66] ELMORE, S. Apoptosis: A Review of Programmed Cell Death. *Toxicologic Pathology*, 35: 495–516, 2007. 10.1080/01926230701320337

[67] Lazebnik, Y. A., KaufmannH, S. H., Desnoyers, S., Poirier, G. G., and Earnshaw, W. C. Cleavage of poly(ADP-ribose) polymerase by a proteinase with properties like ICE *Nature*, 371(6495): 346-347, 1994.

[68] Boulares, A. H., Yakovlev, A. G., Ivanova, V., Stoica, B. A., Wang, G., Iyer, S., and Smulson, M. Role of Poly(ADP-ribose) Polymerase (PARP) Cleavage in Apoptosis. *The journal of biological chemistry*, 274(33): 22932–22940, 1999.

[69] Kastan, M. B., Canman, C. E., and Leonard, C. J. P53, cell cycle control and apoptosis: implications for cancer. *Cancer and Metastasis Reviews*, 14(1): 3-15, 1995.

[70] Shariat, S. F., Ashfaq, R., Sagalowsky, A. I., and Lotan, Y. in *Urologic Oncology: Seminars and Original Investigations.* 468-475 (Elsevier).

[71] Mayo, M. W., Wang, C.-Y., Cogswell, P. C., Rogers-Graham, K. S., Lowe, S. W., Der, C. J., and Baldwin, A. S. Requirement of NF-κB activation to suppress p53-independent apoptosis induced by oncogenic Ras. *Science*, 278(5344): 1812-1815, 1997.

[72] Koyuturk, M., Ersoz, M., and Altiok, N. Simvastatin induces apoptosis in human breast cancer cells: p53 and estrogen receptor independent pathway requiring signalling through JNK. *Cancer letters*, 250(2): 220-228, 2007.

[73] Chopin, V., Toillon, R. A., Jouy, N., and Bourhis, X. L. Sodium butyrate induces P53-independent, Fas-mediated apoptosis in MCF-7 human breast cancer cells. *British journal of pharmacology*, 135(1): 79-86, 2002.

[74] Teng, Y., Ross, J. L., and Cowell, J. K. The involvement of JAK-STAT3 in cell motility, invasion, and metastasis. *Jak-stat*, 3(1): e28086, 2014.

[75] Siddiquee, K. A. Z. and Turkson, J. STAT3 as a target for inducing apoptosis in solid and hematological tumors. *Cell research*, 18(2): 254, 2008.

[76] Devarajan, E. and Huang, S. STAT3 as a central regulator of tumor metastases. *Current molecular medicine*, 9(5): 626-633, 2009.

[77] Yue, P. and Turkson, J. Targeting STAT3 in cancer: how successful are we? *Expert opinion on investigational drugs*, 18(1): 45-56, 2009.

[78] Shi, H. Y., Zhang, W., Liang, R., Abraham, S., Kittrell, F. S., Medina, D., and Zhang, M. Blocking tumor growth, invasion, and metastasis by maspin in a syngeneic breast cancer model. *Cancer research*, 61(18): 6945-6951, 2001.

[79] Pulaski, B. A. and Ostrand-Rosenberg, S. Mouse 4T1 breast tumor model. *Current protocols in immunology*, 39(1): 20.22. 21-20.22. 16, 2000.

[80] Pulaski, B. A. and Ostrand-Rosenberg, S. Mouse 4T1 breast tumor model. *Curr Protoc Immunol*, Chapter20: Unit 20 22, 2001. 10.1002/0471142735.im2002s39

[81] Rashid, O. M., Nagahashi, M., Ramachandran, S., Dumur, C., Schaum, J., Yamada, A., Terracina, K. P., Milstien, S., Spiegel, S., and Takabe, K. An improved syngeneic orthotopic murine model of human breast cancer progression. *Breast cancer research and treatment*, 147(3): 501-512, 2014.

[82] Rashid, O. M. and Takabe, K. Animal models for exploring the pharmacokinetics of breast cancer therapies. *Expert opinion on drug metabolism & toxicology*, 11(2): 221-230, 2015.

[83] Ferraz, A. C., Angelucci, M. E. M., Da Costa, M. L., Batista, I. R., De Oliveira, B. H., and Da Cunha, C. Pharmacological evaluation of ricinine, a central nervous system stimulant isolated from Ricinus communis. *Pharmacology Biochemistry and Behavior*, 63(3): 367-375, 1999.

[84] Ohishi, K., Toume, K., Arai, M. A., Sadhu, S. K., Ahmed, F., Mizoguchi, T., Itoh, M., and Ishibashi, M. Ricinine: a pyridone alkaloid from Ricinus communis that activates the Wnt signaling pathway through casein kinase 1α. *Bioorganic & Medicinal Chemistry*, 22(17): 4597-4601, 2014.

[85] Vieira, C., Evangelista, S., Cirillo, R., Lippi, A., Maggi, C. A., and Manzini, S. Effect of ricinoleic acid in acute and subchronic experimental models of inflammation. *Mediators of Inflammation*, 9(5): 223-228, 2000.

[86] Jaganathan, S. K., Supriyanto, E., and Mandal, M. Events associated with apoptotic effect of p-coumaric acid in HCT-15 colon cancer cells. *World Journal of Gastroenterology: WJG*, 19(43): 7726, 2013.

[87] Xuan, H., Li, Z., Yan, H., Sang, Q., Wang, K., He, Q., Wang, Y., and Hu, F. Antitumor activity of Chinese propolis in human breast cancer MCF-7 and MDA-MB-231 cells. *Evidence-Based Complementary and Alternative Medicine*, 2014, 2014.

[88] Ahmad, N., Feyes, D. K., Agarwal, R., Mukhtar, H., and Nieminen, A.-L. Green tea constituent epigallocatechin-3-gallate and induction of apoptosis and cell cycle arrest in human carcinoma cells. *Journal of the National Cancer Institute*, 89(24): 1881-1886, 1997.